Climate Data Record (CDR) Program

Climate Algorithm Theoretical Basis Document (C-ATBD)

Mean Layer Temperature - NOAA CDR

CDR Program Document Number: CDRP-ATBD-0682
Configuration Item Number: 01B-25
Revision 2 / December 20, 2023

REVISION HISTORY

Rev.	Author	DSR No.	Description	Date
1	Cheng-Zhi Zou and Jian Li NOAA/NESDIS/STAR	DSR-860	Initial Submission to CDR Program	04/06/2015
2	Cheng-Zhi Zou and Xianjun Hao	DSR-1862	Revised Submission to CDR Program for upgrade to v5.0	12/08/2023

TABLE of CONTENTS

LIST of FIGURES

LIST of TABLES

1. Introduction

1.1 Purpose

The purpose of this document is to describe the algorithm submitted to the National Centers for Environmental Information (NCEI) by Cheng-Zhi Zou at NOAA/NESDIS/Center for Satellite Applications and Research (STAR) that will be used to create the NOAA Mean Layer Temperature (MLT) Climate Data Record (CDR) based on satellite microwave sounder observations. Satellite instruments used for the CDR creation included the Microwave Sounding Unit (MSU), Advanced Microwave Sounding Unit-A (AMSU-A), and Advanced Technology Microwave Sounder (ATMS) onboard historical NOAA polar orbiting satellites TIROS-N through NOAA-19, Suomi National Polar-orbiting Partnership (SNPP), NOAA-20, EUMETSAT MetOp-A and NASA Aqua. The actual algorithm is defined by the computer program (code) that accompanies this document, and thus the intent here is to provide a guide to understanding that algorithm, from both a scientific perspective and in order to assist a software engineer or end-user performing an evaluation of the code.

1.2 Definitions

The following is a summary of the phrases and symbols used to define the algorithm.

Mean Layer Temperature (MLT, or Atmospheric Layer Temperature, or Deep-Layer Atmospheric Temperature): Averaged brightness temperatures of those binned into grid cells within a predefined time interval. Because the MSU/AMSU-A/ATMS brightness temperature comes from different levels with different weighting functions within an atmospheric layer, the gridded brightness temperature is thus interpreted as atmospheric layer temperature or mean layer temperature

Brightness Temperature (BT): Satellite observation at the top of the atmosphere at each scan position. It is converted from *Radiance* using the Planck Function with instrument channel frequency as inputs

Radiance: Satellite observation of the radiation emitted to space from the earth and atmosphere. it is converted from raw counts readings of satellite instruments using instrument calibration equation. Refer to 'CDRP C-ATBD: MSU/AMSU Radiance FCDR Derived from Integrated Microwave Inter-Calibration Approach' for derivation of radiances from satellite raw counts data

Bias correction: The original brightness temperatures observed at scan positions are subject to a series of adjustments to derive bias-corrected brightness temperatures for each satellite. These bias-corrected or adjusted brightness temperatures for different satellites are then merged together to derive long-term climate data record. Biases being adjusted included those from calibration drift, incident angle effect, channel frequency differences, diurnal drift, and warm target

temperature effect. The root cause, nature, and adjusting algorithms for these biases are described in detail in the Theoretical Description Section of the algorithms.

Data Types: Three types of data sets are frequently discussed in this document. Unless otherwise specified, these data types are defined as follows:

Level-1C data: Orbital data containing swath radiances at scan positions as well as other satellite geo-location and calibration information taken from the satellite Level-1b files or IMICA recalibrated orbital files or reprocessed ATMS data files

Level-3 data: Gridded dataset generated from Level-1C data for individual satellites. They are the MLT for individual satellites

Merged Mean Layer Temperature Products: Merged Level-3 data products (MLT) from multiple satellites after bias adjustments for all known sources of error

1.3 Referencing this Document

This document should be referenced as follows:

Mean Layer Temperature - NOAA - Climate Algorithm Theoretical Basis Document, NOAA Climate Data Record Program CDRP-ATBD-0682 Rev. 2 (2023). Available https://www.ncei.noaa.gov/products/climate-data-records

1.4 Document Maintenance

This C-ATBD describes the intercalibration and merging algorithms as well as data products characteristics for Version 5.0 of the Mean Layer Temperature - NOAA CDR. The Mean Layer Temperature - NOAA V5.0 CDR includes observations from three generations of satellite microwave sounders (MSU, AMSU-A, and ATMS) onboard 16 polar-orbiting satellites. The MSU satellites included TIROS-N, NOAA-6, NOAA-7, NOAA-8, NOAA-9, NOAA-10, NOAA-11, NOAA-12, and NOAA-14. The MSU observations stopped in 2007 and they were replaced by their successor, the AMSU-A, since 1998. The AMSU-A satellites used in Mean Layer Temperature - NOAA CDR v5.0 include NOAA-15, -18, -19, MetOp-A, and EOS Aqua. Observations from ATMS are available since 2012 onboard SNPP and NOAA-20 which are also used in Mean Layer Temperature - NOAA CDR v5.0. Figure 1-1(a) and Figure 1-1(b) show timelines for these satellites and local equator crossing time (LECT), respectively. Most of these satellites are still operating at the time of this writing, and new observations are being added to the existing dataset every month. Recalibration and merging algorithms for generating the MLT CDR from the MSU, AMSU-A, and ATMS measurements were based on the current understanding of the data issues and bias characteristics of the observations. New data issues and improved understanding of the old data issues may often occur when new observations become available. As such, algorithm updates and data version upgrade

will be expected for the merged MSU/AMSU-A/ATMS data products in the future which may result in improved understanding of the atmospheric temperature trends. If a substantial change occurs, the document will be rewritten to incorporate algorithm updates and new findings.

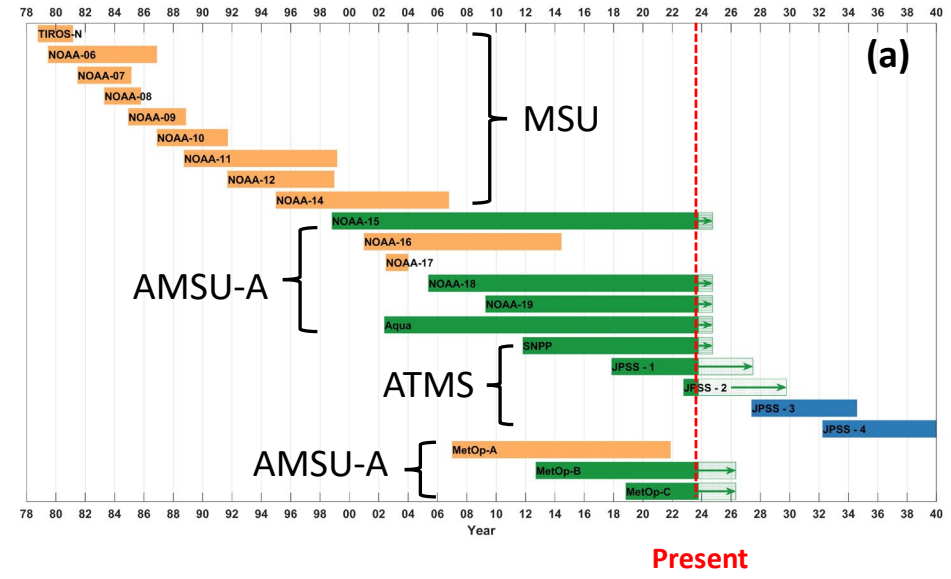

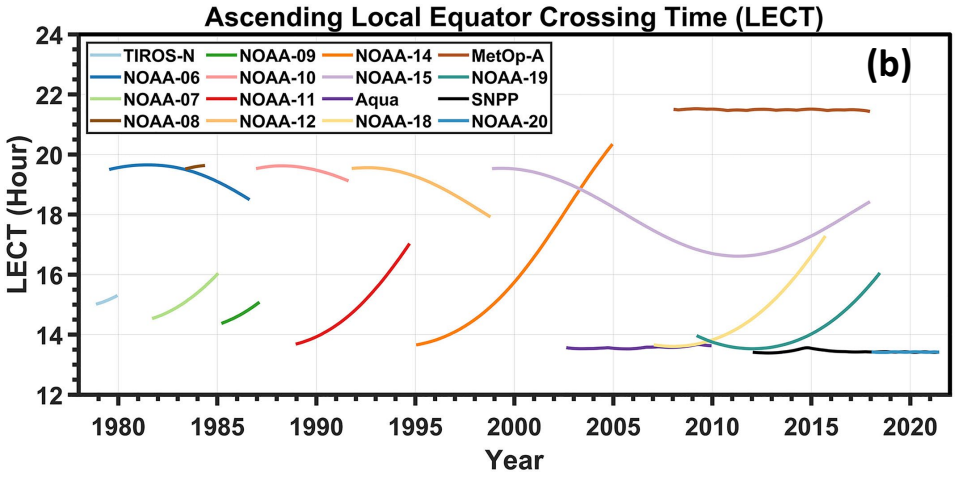

Figure 1-1. a) Timelines for the MSU, AMSU-A, and ATMS satellites; b) Ascending Local Equator Crossing Time (LECT) for satellites used in Mean Layer Temperature - NOAA CDR v5.0.

2. Observing Systems Overview

2.1 Products Generated

Three channel-based, monthly gridded MLT CDR are generated by using merging algorithms described in this document and previous publications. These are temperatures of middle-troposphere (TMT), upper-troposphere (TUT), and lower-stratosphere (TLS), corresponding to measurements from the MSU channels 2, 3, and 4 and their companion AMSU-A channels 5, 7, and 9, ATMS channels 6, 8, and 10, respectively. In addition, the temperature of lower-troposphere (TLT) is generated using a combination of TMT, TUT, and TLS. The combination coefficients are provided in the algorithm sections. Table 2-1 lists the vertical coverage and spatial resolution of these products. They are derived from 16 polar orbiting satellites including TRIOS-N, NOAA-6 through NOAA-19, EUMETSAT MetOp-A, NASA Aqua, SNPP, and NOAA-20 covering the time period from November 1978 to present.

Table 2-1. Products generated in this CDR. These are 44+ year-long, global monthly datasets with 2.5° latitude by 2.5° longitude grid resolution

Data Products (Global Monthly)	*Acronym*	*Spatial resolution*	*Time Period*	*Microwave Sounding Channel*	Vertical Layer Coverage	*Peaking Level*
Temperature Mid-Troposphere	TMT	2.5^0 latitude by 2.5^0 longitude	11/1978–present	MSU Ch2/AMSU-A Ch5/ATMS Ch6	Surface-17km	5 km
Temperature Upper-Troposphere	TUT	2.5^0 latitude by 2.5^0 longitude	01/1981–present	MSU Ch3/AMSU-A Ch7/ATMS Ch8	3-20 km	10 km
Temperature Lower-Stratosphere	TLS	2.5^0 latitude by 2.5^0 longitude	12/1978–present	MSU Ch4/AMSU-A Ch9/ATMS Ch10	12-26km	17 km
Temperature Lower-Troposphere	TLT	2.5^0 latitude by 2.5^0 longitude	01/1981–present	Combinations from TMT, TUT, and TLS	Surface-12km	3 km

2.2 Instrument Characteristics

MSU and AMSU-A are both cross-track, line-scanned instruments designed to measure Earth radiation emitted by the atmospheric oxygen for temperature sounding. The detailed system parameters and measurement principles for MSU and AMSU-A can be found in Kidwell (1998) and Robel and Graumann (2014). The ATMS is a total power cross-track radiometer with 22 channels, providing sounding observations of the atmospheric temperature and moisture profiles. Weng et al. (2012) and Goldberg et al. (2013) described the ATMS system parameters and measurement principles in detail. The following subsections only summarize characteristics of these instruments relevant to the satellite intercalibration and TCDR development.

2.2.1 MSU

The MSU on board NOAA polar orbiting satellite series had been the primary instruments for measuring upper-air temperature profiles under all weather conditions, excluding precipitation, during 1978-2007. MSU was a microwave radiometer with four-channels to make passive measurements in the 5.5 millimeter oxygen region. The four channels responded to the following spectral frequencies: 50.3, 53.74, 54.96, and 57.95 GHz, respectively, with a channel bandwidth of 200 MHz in each case and a typical noise equivalent differential temperature (NEΔT) of 0.3K. The radiance measured by each frequency channel comes from a different layer of the atmosphere, depending on the strength of the absorption at that frequency. The relative contribution of temperatures at individual levels to the measured layer temperature is represented by a vertical weighting function, which is typically a bell-shaped curve peaking at a certain altitude (Figure 2-1; the lower parts of the near surface channels are often cut off by the surface). Among these, MSU channel 1 (50.3 GHz) measured surface temperature, and channels 2, 3 and 4 measured TMT, TUT, and TLS with their weighting functions peaking respectively near 5, 12, and 17 km (Figure 2-1).

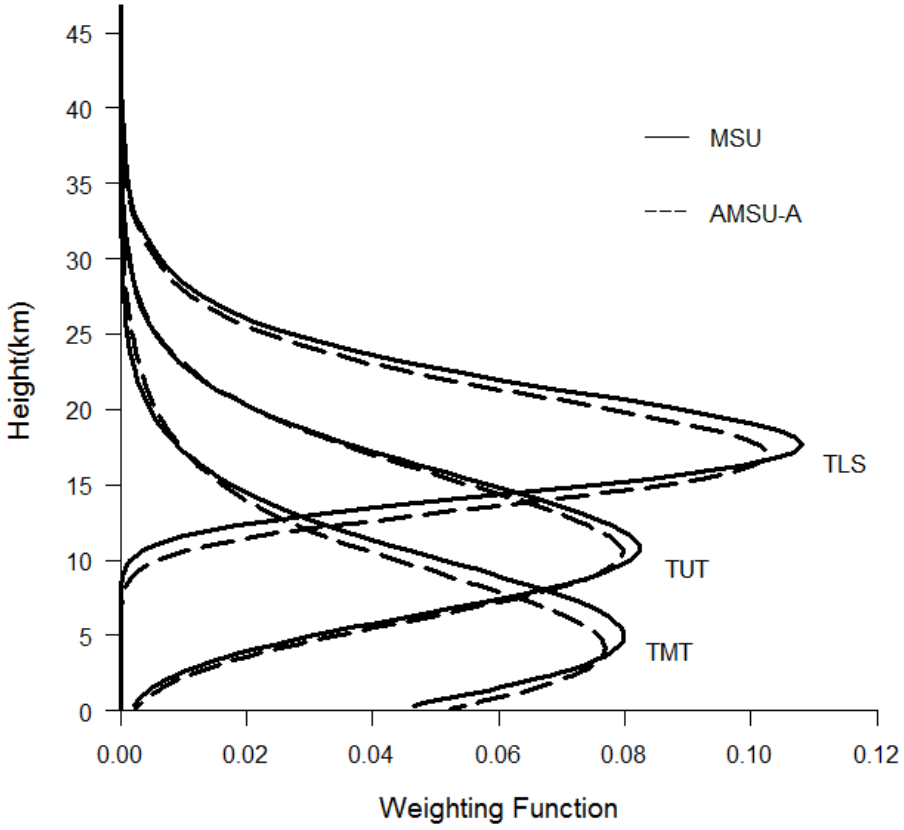

Figure 2-1. Weighting functions for the three MSU (solid lines) and AMSU-A (dashed lines) channels that measure temperatures of the mid-troposphere (TMT), upper-troposphere (TUT), and lower-stratosphere (TLS). The weighting functions correspond to nadir observing conditions for the US standard atmospheric temperature profile. The ATMS weighting functions for TMT, TUT, and TLS are the same as the AMSU-A weighting functions since their channel frequencies are exactly the same.

The MSU was flown on nine sequential NOAA polar-orbiting satellites, TIROS-N through NOAA-14 (Figure 1-1). The MSU made eleven Earth observations during each cross-track scan. The MSU sensors consisted of two four-inch diameter antennas named as MSU-1 and MSU-2. Each of the two antennas had an Instantaneous Field of View (IFOV) of 7.5 degrees. The MSU-1 was used by channels 1 and 2 while MSU-2 by channels 3 and 4. The antennas were step scanned through the eleven individual Earth views with each step taking 1.84 seconds. It required a total of 25.6 seconds to complete eleven scans. The MSU instrument parameters are summarized in Table 2-2.

Table 2-2. MSU instrument parameters

Cross-track scan angle (degree from nadir)	±47.35
Scan time (second)	25.6
Number of steps	11
Angular FOV (degree)	7.5
Step angle (degree)	9.47
Step time (second)	1.84
Ground IFOV at nadir (km diameter)	109.3
Ground IFOV at end of scan	323.1 km cross-track 178.8 km along-track
Distance between IFOV centers (km along-track)	168.1
Swath width (km)	±1174
Time between start of each scan line (second)	25.6
Step and dwell time (second)	1.81
Time difference between the start of each scan and the center of the first dwell period (second)	0.9
Total channels	4
Channel frequencies (GHz) and polarization (Vertical versus Horizontal)	CHs 1 2 3 4 Frequency 50.30 53.74 54.96 57.95 Polarization V H V H
Instrument antenna systems	MSU-1 and MSU-2
Responsible antennas for each channel	MSU-1 for channels 1 and 2 MSU-2 for channels 3 and 4
Channel bandwidth (MHz)	200
Black body and space view per scan line	1
PRTs on each warm target	2

2.2.2 AMSU-A

Since 1998, AMSU-A onboard NOAA-15 and its follow-on satellites has replaced MSU. As a successor to MSU, AMSU-A has improved instrument accuracy, and with its 15 channels provides finer vertical resolution and measurements well into the upper stratosphere. The AMSU-A antenna beam-width is 3.3 degrees at each channel frequency. There are thirty Earth views in each scanline every eight seconds, covering 48.33 degrees on each side of the nadir direction. These scan patterns and geometric resolution translate to a 45 km diameter cell at nadir and a 2,343 km swath width from the 833 km nominal orbital altitude. Among all discrete

frequency channels, channels 5, 7, and 9 share a similar spectrum frequency with MSU channel 2, 3, and 4, respectively [Figure 2-1]. The Mean Layer Temperature - NOAA CDR v5.0 CDR uses a backward merging approach, meaning the earlier MSU observations are adjusted to the later AMSU-A observations. As such, frequency adjustment on each individual MSU channels is conducted to obtain equivalent AMSU-A channels which are then merged with the three AMSU-A channels to produce MLTs. Detailed frequency adjustment algorithms are described shortly in the merging algorithm section. Table 2-3 and Table 2-4 summarize the AMSU-A instrument parameters.

Table 2-3. AMSU-A instrument parameters

Cross-track scan angle (degree from nadir)	±48.33			
Scan time (second)	5.965			
Number of steps	30			
Step angle (degree)	3.33			
Step time (second)	0.1988			
Ground IFOV at nadir (km diameter)	45			
Swath width (km)	±1171			
Time between start of each scan line (second)	8			
Step and dwell time (second)	0.1988			
Total channels	15			
Channel Frequencies (GHz) and polarization (Vertical versus Horizontal)	CHs:	5	7	9
	Frequency	53.60	54.94	57.29
	Polarization	H	V	H

Table 2-4. Channel and scanning view parameters for each AMSU-A antenna systems.

Instrument Antenna Systems	**A1-1**	**A1-2**	**A2**
Channel	6-7,9-15	3-5,8	1-2
Earth views per scan line	30	30	30
Blackbody and space view per scan line	2	2	2
PRTs in each warm target	5	5	7

2.2.3 ATMS

The ATMS is a total power cross-track radiometer with 22 channels, combining all the channels of the heritage sensors, including AMSU-A and AMSU-B/Microwave Humidity Sounder (MHS), into a single sensor that spans from 23 to 183 GHz (Table 2-5). Such a design offers significant advantage in the reduction in instrument weight and the use of power. Among the channels, 1–2 and 16–17 are the window channels providing information on the atmospheric clouds, total precipitable water, surface emissivity, and water vapor concentration near the surface. Channels 3–15 are the oxygen channels for temperature soundings from the surface to the upper stratosphere at approximately 1 hPa. The remaining channels, 18–22, use water vapor absorption lines at 183 GHz for humidity soundings from the lower to the upper troposphere at about 200 hPa. The ATMS channel frequencies are the same as those of AMSU-A and AMSU-B/MHS for most channels except for the addition of temperature-sounding channel 4 (51.76 GHz) and two water vapor channels at 183 GHz. Table 2-5 listed basic characteristics for ATMS channels 6, 8, and 10, which are companion channels for AMSU-A channels 5, 7, and 9, respectively, for development of the Mean Layer Temperature - NOAA CDR v5.0 CDR.

Table 2-5. Basic characteristics for the Advanced Technology Microwave Sounder (ATMS) channels. The abbreviations QV and QH refer to quasi-vertical and quasi-horizontal, respectively.

ATMS Channel	Center Frequency (MHz)	Polarization	Maximum Bandwidth (MHz)	Calibration Accuracy (K)	3-dB Bandwidth (deg)	Reference Channels
6	53,596 ± 115	H	170	0.75	2.2	AMSU-A Ch5
8	54,940	H	400	0.75	2.2	AMSU-A Ch7
10	57,290.344(f_0)	H	330	0.75	2.2	AMSU-A Ch9

The ATMS has two receiving antennas—one serving channels 1–15 and the other serving channels 16–22. ATMS scans the Earth within the range of 52.725° on each side of the nadir direction with an angular sampling interval of 1.11°, providing 96 Earth observations in a scan line with a swath width about 2600 km. Each of the 96 Earth samples takes about 18 milliseconds integration time. The beam width of the scans is 2.2° for channels 3–16. This gives a ground nadir field of view (FOV) resolution of 32 km for channels 3–16 for the SNPP orbital height of 829 km above the Earth. The beam width differences between ATMS and AMSU-A result in differences in the size of their FOVs. Because the angular sampling interval is much smaller than the beam width, the ATMS scans result in oversampling in both cross-track and along-track directions. A single FOV of any of ATMS channels 3 to 16 typically overlaps with its three neighboring FOVs and three nearby scan lines. The oversampling in the ATMS observations offers an advantage in the generation of the climate data record—sampling noise can be much reduced when multiple samples are averaged together to generate a single observation to represent a climate state.

3. Algorithm Description

3.1 Algorithm Overview

The main purpose of the merging algorithm is to derive homogeneous MLT CDR from the sequential overlapping MSU, AMSU-A, and ATMS observations onboard NOAA/EUMETSAT/NASA/SNPP/JPSS polar orbiting satellites channel by channel. The Mean Layer Temperature - NOAA CDR v5.0 used a merging approach very different from previous versions of the STAR MLT datasets. This new approach is referred to as 'backward merging approach' in which satellite merging started from the latest backward to the earlier ones. A time series during 2002-present was used as a reference in the backward merging, which was based on satellite microwave sounder observations in stable sun-synchronous orbits. The reference time series has a high accuracy in trend detection, allowing intercalibration and trend detection with better accuracy in time series of the entire period from 1979 to present. The high accuracy of the reference time series was discussed in Zou et al. (2018, 2021) and the backward merging approach was described in detail in Zou et al. (2023). In addition, the Level-1c radiance data used for deriving the MLT CDR was already inter-calibrated by Zou and Wang (2011, 2013) using the Integrated Microwave Inter-Calibration Approach (IMICA), formerly known as the simultaneous nadir overpass approach. Limb-adjusted brightness temperatures from MSU observations were provided in the IMICA calibrated Level-1c files. The IMICA calibrated MSU and AMSU-A radiances and limb adjustments for MSU were described in detail in the C-ATBD associated with the MSU and AMSU-A Level-1c radiances dataset (Zou and Wang 2013). In Mean Layer Temperature - NOAA CDR v5.0 CDR, some satellite channels were recalibrated again to remove their calibration drifting errors found in recent years. This will be described in more detail in later sections. For most satellite channels, however, the IMICA inter-calibrated radiances were still used in the creation of Mean Layer Temperature - NOAA CDR v5.0. This has substantially simplified the processing procedure for creating Mean Layer Temperature - NOAA CDR v5.0. The following provides a summary on the steps and algorithms needed to create the Mean Layer Temperature - NOAA CDR v5.0. Detailed steps can also be found in the flowcharts shown in Figures 3-1 and 3-2.

- Create reference MLT time series using satellite observations only in stable sun-synchronous orbits
- Extract IMICA-calibrated, limb-adjusted MSU swath brightness temperatures for channels 2, 3 and 4 from the IMICA calibrated MSU orbital Level-1c datasets
- Extract IMICA-calibrated (without limb adjustment) AMSU-A swath brightness temperatures for channels 5, 7 and 9 from the IMICA calibrated AMSU-A orbital Level-1c datasets
- Recalibrate some old satellite channels to remove their calibration drifting errors
- Adjust observations made at different viewing angles to nadir views

- Conduct channel frequency adjustment for MSU observations to derive AMSU-A/ATMS equivalent MSU observations
- Conduct diurnal drift adjustment using a semi-physical model developed by Zou et al. (2023)
- Remove instrument temperature effects on observations
- Bin limb-, frequency-, diurnal-, and instrument temperature effect-adjusted brightness temperatures at scan positions into grid cells of 2.5^{o}x2.5^{o} spatial resolution in monthly interval for each satellite and then average them to produce the Level-3 mean layer temperature data for each satellite
- Average overlapping satellites at each grid cells to create a 44-year long, merged and homogeneous global layer temperature CDR from 1978 to present. This was done for each channel separately.

3.2 Processing Outline

This section provides a general description of the MSU/AMSU-A/ATMS MLT production system with a set of multiple flowcharts.

3.2.1 Overall Processing Outline

The overall processing outline of the Mean Layer Temperature - NOAA CDR v5.0 is summarized in Figure 3-1. Each of the components is described in the following subsections.

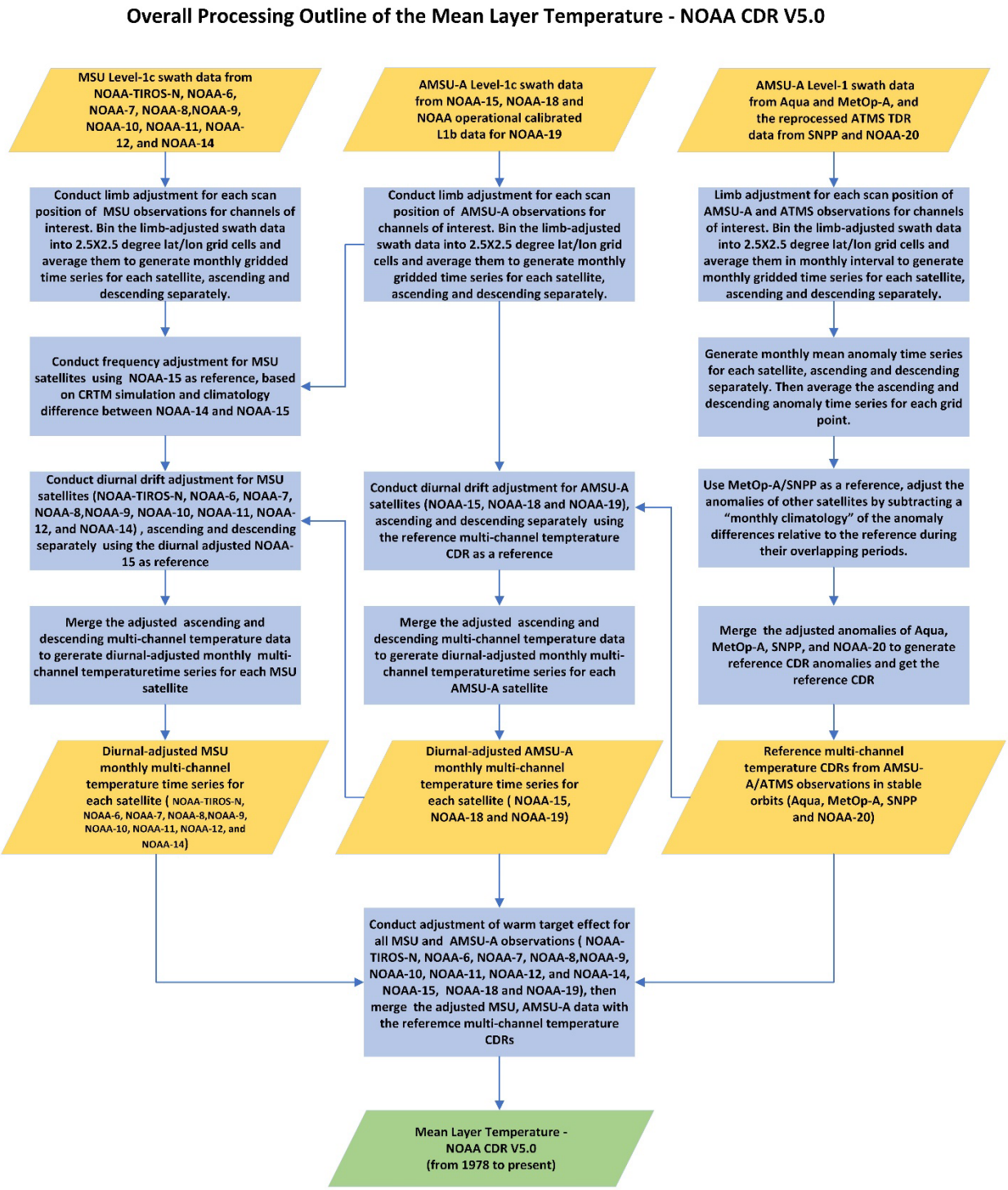

Figure 3-1. High level flowchart of the Mean Layer Temperature - NOAA CDR v5.0 algorithm illustrating the main processing section.

3.2.2 System Configuration

The system configuration is designed separately for the generation of level 3 layer temperatures of individual satellites and their merged products (Figures 3-2 (a) and (b). Both configurations are common in setting I/O directories and ancillary data directory.

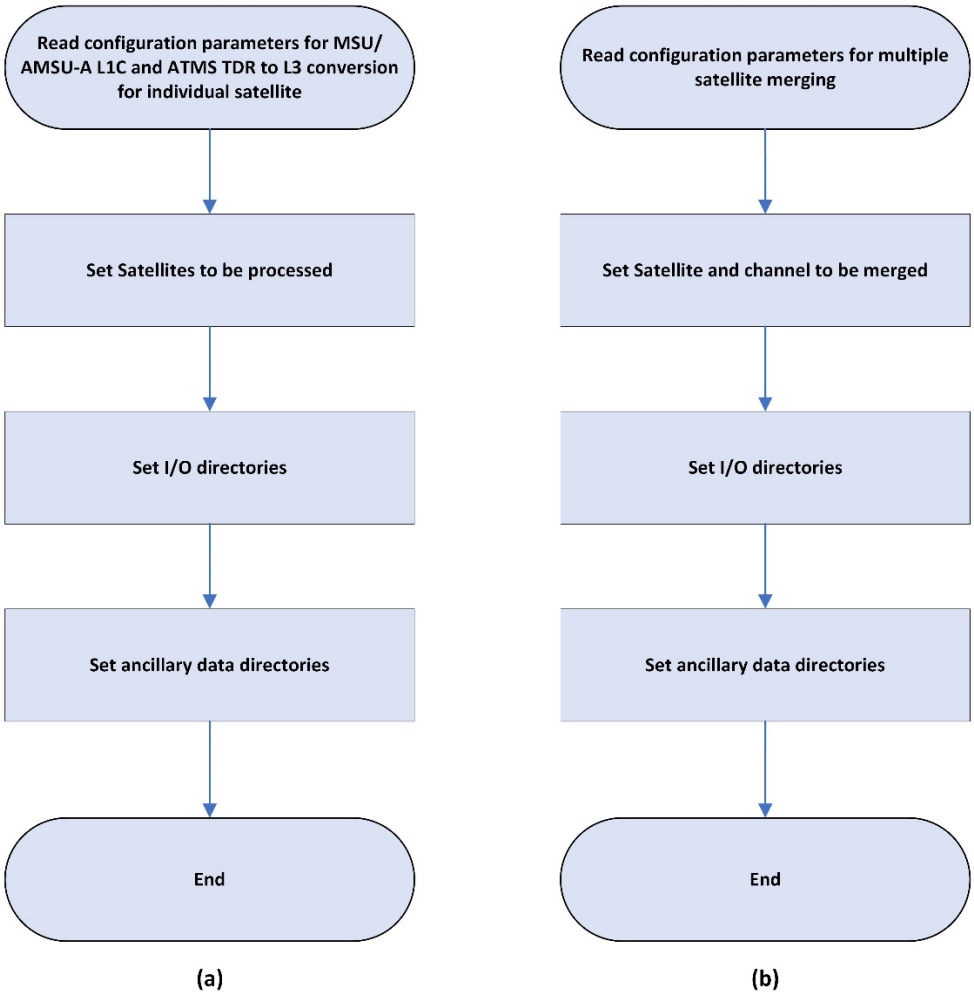

Figure 3-2. Input parameter configuration flowcharts for (a) generation of level-3 data of individual satellites and (b) generation of merged MLT for different channels

For generation of Level 3 data of individual satellites, the processing uses level-1c files of individual satellites, therefore, satellite names need to be specified and multi thread technique is applied to accelerate the production. Merged product contains TMT, TUT, and TLS derived from MSU channels 2, 3, and 4, AMSU-A channels 5, 7, and 9, and ATMS channels

6, 8, and 10, respectively. These are achieved by setting the channel parameter in the system configuration.

3.2.3 Preparing Ancillary Data

Ancillary data include the land-sea fraction data, the look-up table for MSU frequency adjustment, and the look-up tables for MSU/AMSU-A/ATMS limb adjustment.

- Land-sea fraction data: It is required for production of both Level-3 data of individual satellites and their merged products.
- Look-up table for MSU frequency adjustment: It is required to adjust MSU level 3 data to equivalent AMSU-A channels.
- Look-up tables for MSU/AMSU-A/ATMS limb adjustment: these tables are required to adjust MSU/AMSU-A and ATMS measurements of off-nadir pixels to equivalent nadir observations. Limb adjusted MSU data were already included in its IMICA recalibrated datasets.

3.2.4 Converting MSU/AMSU-A Level-1C and ATMS TDR Data to Level-3 Gridded Data

The IMICA calibrated Level-1c data are stored in separated NetCDF files for each orbit. Each file contains necessary information required for MLT CDR generation such as satellite ID, observation time, geo-location records, warm target temperatures, scene temperatures, quality control flags, etc.

ATMS TDR and geolocation data are stored in separate HDF5 files for each granule. Each geolocation file contains information about satellite ID, observation time, geolocation, etc., and each TDR file contains information about scene temperatures, quality control flags, etc.

Figure 3-3 illustrates how to use the data and information in MSU/AMSU-A Level-1c and ATMS TDR data to generate gridded monthly temperature data (Level-3) for each individual satellite.

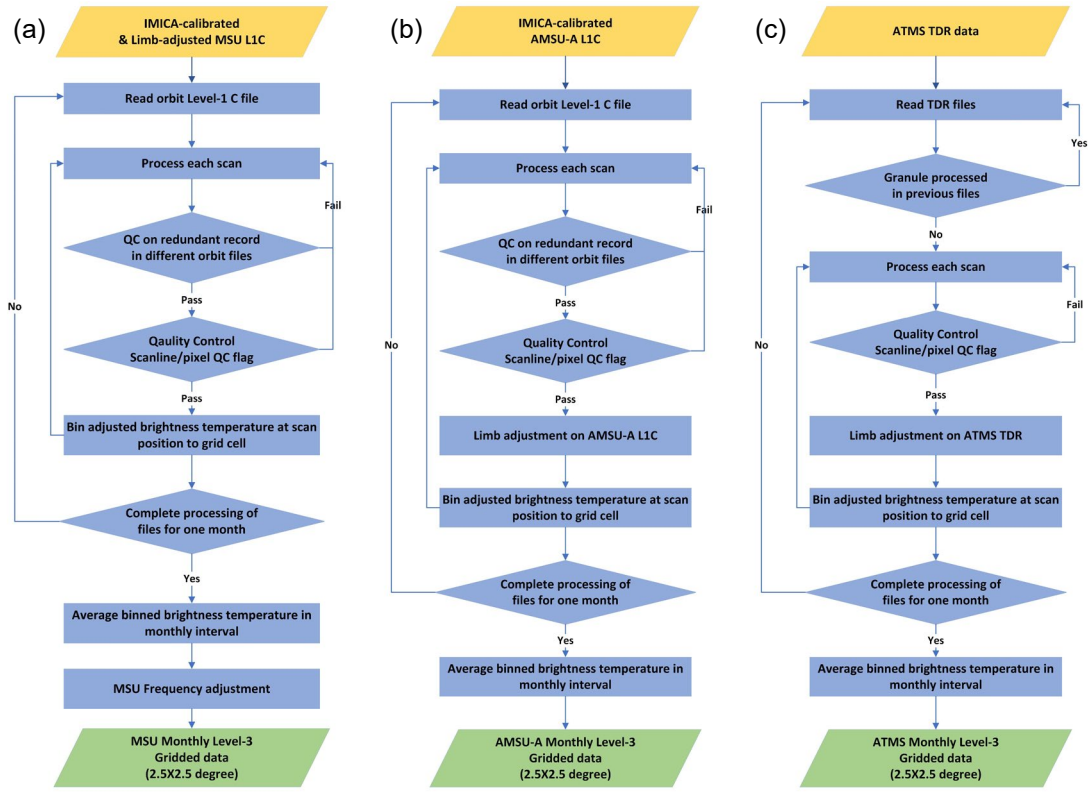

Figure 3-3. Flowchart for processing (a) IMICA recalibrated MSU Level-1c, (b) IMICA recalibrated Level-1c, and (c) reprocessed ATMS TDR brightness temperatures to generate Level-3 gridded monthly temperature records for individual satellites

3.2.5 Generating Reference Multi-channel MLT CDRs

The reference multi-channel temperature time series data were developed using satellites in stable orbits only, which can be used as a reference measurement in diurnal drift adjustment and climate trend detection (Zou et al. 2021). Figure 3-4 illustrates how to use the AMSU-A onboard Aqua and MetOp-A satellites, and the ATMS TDR data onboard SNPP and NOAA-20 satellites to generate references for multi-channel MLT CDRs (Reference TMT or RTMT, Reference TUT or RTUT and Reference TLS or RTLS).

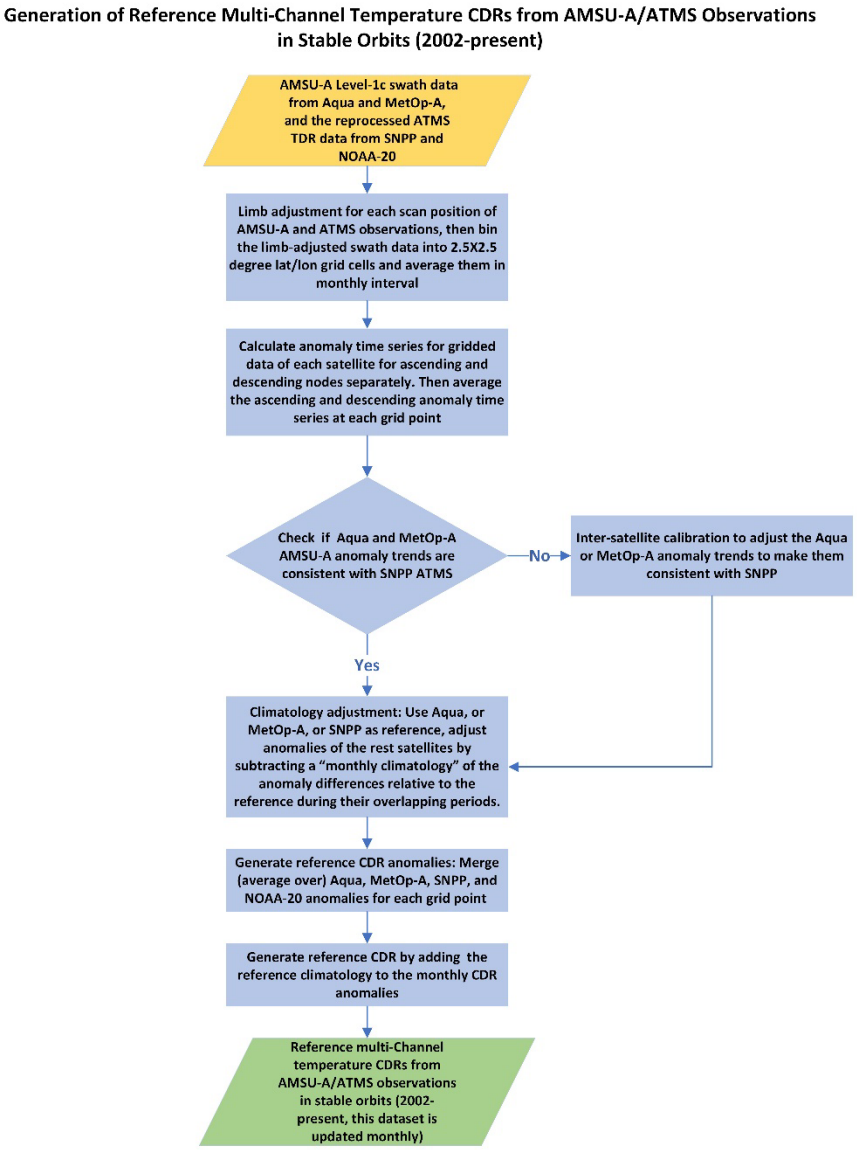

Figure 3-4. Flowchart for generating reference multi-channel temperature CDRs.

3.3 Algorithm Input

3.3.1 Primary Sensor Data

The primary sensor data used to derive the Mean Layer Temperature - NOAA CDR v5.0 includes brightness temperatures in swath format from three types of calibration and recalibration procedures. The first one is based on pre-launch operational calibration that uses thermal-vacuum chamber test to derive calibration coefficients (Mo 1995, 1996). This type of data includes NOAA-19 AMSU-A level-1 radiance that was downloaded from the NOAA Comprehensive Large Array-data Stewardship System (CLASS) archive (https://www.avl.class.noaa.gov/saa/products/welcome). The second one is the IMICA recalibrated brightness temperature FCDR. There are two versions of FCDR in this type of data. Version 1 (V1) FCDR was developed by Zou et al. (2006, 2009, 2010) for MSU and Zou and Wang (2011) for AMSU-A. These data were downloaded from the NOAA NCEI CDR website: https://www.ncei.noaa.gov/products/climate-data-records/fundamental). Detailed characteristics of the V1 FCDR can be found in the C-ATBD for the NOAA MSU/AMSU FCDR (Zou and Wang 2013) available from the NCEI CDR website (https://www.ncei.noaa.gov/pub/data/sds/cdr/CDRs/AMSU%20Brightness%20Temperatures/AlgorithmDescription_01B-18_18a.pdf). Version 2 (V2) FCDR was developed recently (Zou et al. 2023). Version 2 FCDR removed calibration drift for selected MSU/AMSU-A satellite channels based on new reference observations that were unavailable during the development of V1 FCDR. The detailed description for the recalibration of MSU channel 2 and AMSU-A channel 5 for V2 FCDR can be found in Zou et al. (2023). Tables 3-1 and 3-2 list level-1 calibration coefficients for V1 and V2 FCDRs, respectively, for recalibrated MSU satellite and channels. Tables 3-3 and 3-4 provide level-1 calibration coefficients for V1 and V2 FCDRs, respectively, for recalibrated AMSU-A satellites and channels. Tables 3-1 and 3-3 were provided before in the C-ATBD document for the NOAA MSU/AMSU V1 FCDR (Zou and Wang 2013). Here they are listed again for the purpose of completion of this document. The meaning of these calibration coefficients is discussed in the instrument recalibration section in this document.

Table 3-1. Calibration coefficients for Version 1 MSU FCDR for recalibrated satellite channels. The coefficients were obtained from SNO regressions, where δR is the offset and μ the nonlinear coefficient. Units for δR and μ are 10^{-5} (mW) (sr m^2 cm^{-1}) $^{-1}$ and (sr m^2 cm^{-1}) $(mW)^{-1}$, respectively.

Satellite	Channel 2		Channel 3		Channel 4	
	δR	μ	*δR*	μ	*δR*	μ
NOAA TIROS-N	1.3963	5.4062	5.7535	1.2941	1.6808	4.8256
NOAA 6	0	7.3750	0.1162	6.1974	-1.5438	6.5032
NOAA 7	0	7.4380	-2.8131	10.4644	-1.9660	6.5637
NOAA 8	-1.3750	8.2636	1.4737	4.4531	-0.5083	5.5242

NOAA 9	-0.0771	5.9713	0.1026	9.0332	0.7721	6.1028
NOAA 10	0	6.2 500	0	5.6300	0	4.9500
NOAA 11	-2.4641	9.5909	-1.9983	7.1892	-0.7271	5.4574
NOAA 12	-0.0996	6.7706	-2.3979	8.3282	-4.6074	7.1040
NOAA 14	-0.6363	7.4695	-3.0810	8.7524	-0.7753	5.4175

Table 3-2. Calibration coefficients for Version 2 MSU channel 2 FCDR for recalibrated satellites. The coefficients were obtained using SNO regressions. For simplicity, all δR_0 and μ_0 were adjusted to a reference time of t0=2001 and t1=1998. Units for δR_0, μ_0, κ and λ are 10^{-5} (mW) (sr m^2 cm^{-1}) $^{-1}$, (sr m^2 cm^{-1}) (mW)$^{-1}$, 10^{-5} (mW) (sr m^2 cm^{-1}) $^{-1}$ (year)$^{-1}$ and (sr m^2 cm^{-1}) (mW)$^{-1}$(year)$^{-1}$, respectively.

Satellite	δR_0	k	μ_0	λ
NOAA-14	2.136	-0.118	7.156	-0.139
NOAA-12	1.772	-0.101	6.588	-0.102
NOAA-11	4.259	-0.064	9.592	-0.047
NOAA-10	2.841	-0.018	6.513	-0.015
NOAA-9	2.944	0.0	5.9714	0.0
NOAA-8	1.177	0.0	7.5141	0.0
NOAA-7	3.021	0.0	6.6502	0.0
NOAA-6	2.699	0.0	7.3750	0.0
TIROS-N	4.317	0.0	5.4062	0.0

Table 3-3. Calibration coefficients for Version 1 AMSU-A FCDR for recalibrated satellite channels. The coefficients were obtained from SNO regressions. For simplicity, all δR and μ were adjusted to the corresponding starting time shown in the calibration equation (2001 for δR and 1998 for μ). Units for δR_0, μ_0, κ, and λ are 10^{-5} (mW) (sr m^2 cm^{-1})$^{-1}$, (sr m^2 cm^{-1}) (mW)$^{-1}$, (mW) (sr m^2 cm^{-1})$^{-1}$ (year)$^{-1}$, and (sr m^2 cm^{-1}) (mW)$^{-1}$(year)$^{-1}$, respectively.

		δR_0	κ	μ_0	λ
Channel 4	NOAA-15	0	0	-0.269	0
	NOAA-16	0	0	-0.718	0
	NOAA-17	0.220	0	-0.886	0
	NOAA-18	0.276	0	0.929	0
	MetOp-A	0.324	0	0.442	0
	Aqua	-0.034	0	0	0

Channel 5	NOAA-15	0	0	0.3	0
	NOAA-16	-1.846	-7.248e-07	2.4	0
	NOAA-17	0.877	0	-1.007	0
	NOAA-18	0	0	1.468	0
	MetOp-A	0.467	0	0.262	0
	Aqua	0.023	0	0	0
Channel 6	NOAA-15	1.406	-0.614e-05	0	0.442
	NOAA-16	-2.903	-1.177e-06	4.3	0
	NOAA-17	5.065	0	-3.722	0
	NOAA-18	0	0	3	0
	MetOp-A	1.131	0	2.389	0
	Aqua	1.667	0	0	0
Channel 7	NOAA-15	0	0	0.3	0
	NOAA-16	-4.475	-1.570e-06	3.6	0
	NOAA-17	3.043	0	-2.347	0
	NOAA-18	1.319	0	0.479	0
	MetOp-A	2.152	-1.169e-06	0.396	0
	Aqua	-0.341	0	0	0
Channel 8	NOAA-15	0	0	0.667	0
	NOAA-16	-5.043	-1.768e-06	4.3	0
	NOAA-17	2.078	0	-1.099	0
	NOAA-18	0.440	0	0.964	0
	MetOp-A	1.633	0	0	0
	Aqua	-0.034	0	0	0
Channel 9	NOAA-15	0	0	0.077	0
	NOAA-16	-4.130	-3.936e-07	2.3	0
	NOAA-17	1.334	0	-0.809	0
	NOAA-18	-0.108	0	0.820	0
	MetOp-A	0.111	0	1.246	0
	Aqua	-1.403	0	0	0
Channel 10	NOAA-15	0	0	0.346	0
	NOAA-16	0.227	0	-0.200	0
	NOAA-17	0.711	0	-0.361	0
	NOAA-18	0.876	0	1.116	0
	MetOp-A	0.975	0	1.148	0
	Aqua	-0.189	0	0	0
Channel 11	NOAA-15	0.532	0	0.251	0
	NOAA-16	-0.788	2.910e-7	0.733	0

	NOAA-17	0.595	0	0.406	0
	NOAA-18	0	0	1.500	0
	MetOp-A	0.614	0	1.626	0
	Aqua	0	0	0	
Channel 12	NOAA-15	0	0	1.115	0
	NOAA-16	-0.300	-8.000e-7	1.600	0
	NOAA-17	1.752	0	0	0
	NOAA-18	3.390	0	0	0
	MetOp-A	3.662	0	0	0
	Aqua	1.754	0	0	0
Channel 13	NOAA-15	0	0	1.500	0
	NOAA-16	0.702	-8.045e-07	1.000	0
	NOAA-17	1.471	0	0	0
	NOAA-18	3.171	0	0	0
	MetOp-A	3.018	0	0	0
	Aqua	2.696	0	0	0
Channel 14	NOAA-15	0	0	0	0
	NOAA-16	-1.364	-0.154e-5	1.200	0
	NOAA-17	-0.514	0	0.712	0
	NOAA-18	0	0	0.600	0
	MetOp-A	-0.062	0	-0.435	0
	Aqua	0	0	0	0

Table 3-4. Calibration coefficients for Version 2 AMSU-A FCDR for recalibrated satellite channels. The coefficients were obtained from SNO regressions. For simplicity, all δR_0 and μ_0 were adjusted to a reference time of t0=2001 and t1=1998. Units for δR_0, μ_0, κ, and λ are 10^{-5} (mW) (sr m^2 cm^{-1})$^{-1}$, (sr m^2 cm^{-1}) (mW)$^{-1}$, (mW) (sr m^2 cm^{-1})$^{-1}$ (year)$^{-1}$, and (sr m^2 cm^{-1}) (mW)$^{-1}$(year)$^{-1}$, respectively.

	Satellite	δR_0	k	μ_0	λ
Channel 4	Metop-A	0.0	0.0	0.0	0.0
	NOAA-15	-0.043	0.01	-1.088	0.026
	NOAA-18	0.178	0.0	0.426	0.0
	NOAA-19	0.456	0.0	0.750	0.0
Channel 5	Metop-A	0.0	0.0	0.0	0.0
	NOAA-15	-0.442	0.112	-1.253	0.126
	NOAA-18	1.056	-0.071	3.083	-0.150
	NOAA-19	0.617	0.0	0.752	0.0
Channel 6	Metop-A	0.0	0.0	0.0	0.0

	NOAA-15	1.646	-0.081	1.089	-0.18
	NOAA-18	-0.274	0.0	0.120	0.0
	NOAA-19	-0.024	0.0	0.056	0.0
Channel 9	Metop-A	0.0	0.0	0.0	0.0
	NOAA-15	-0.390	0.011	-0.657	-0.006
	NOAA-18	1.347	-0.105	1.446	-0.091
	NOAA-19	0.555	-0.059	0.837	-0.046
Channel 10	Metop-A	0.0	0.0	-0.25	0.0
	NOAA-15	0.519	0.0	-0.571	0.0
	NOAA-18	1.272	-0.1080	1.632	-0.089
	NOAA-19	-0.228	0.0	-0.297	0.0

The third type of data used in Mean Layer Temperature - NOAA CDR v5.0 is the reprocessed ATMS Temperature Data Record (TDR) from the JPSS satellite series (SNPP and NOAA-20). The ATMS reprocessing was described in detail in Zou et al. (2020) and the reprocessed ATMS TDR data was downloaded from the NOAA CLASS archive (https://www.avl.class.noaa.gov/saa/products/welcome). Table 3-5 provides a detailed list of all the satellites, channels, data time periods, and data types used in the development of Mean Layer Temperature - NOAA CDR v5.0. Note that different channels may come from different data types and undergo different time periods even for the same satellite.

Table 3-5. Satellite periods and data types of the input primary sensor data used for developing the Mean Layer Temperature - NOAA CDR v5.0. The input data are brightness temperatures in orbital swath format for MSU channels 2/3/4, AMSU-A channels 5/7/9, and ATMS channels 6/8/10. The acronyms V1, V2, OP, and RP stand for Version 1 IMICA FCDR, Version 2 IMICA FCDR, Operational calibrated level-1 radiance, and reprocessed TDRs, respectively.

Satellite/Sensor	Time Period (TMT) MSU Ch2; AMSU-A Ch5; ATMS Ch6	Time Period (TUT) MSU Ch3; AMSU-A Ch7; ATMS Ch8	Time Period (TLS) MSU Ch4; AMSU-A Ch9; ATMS Ch10
TIROS-N/MSU	11/1978 to 12/1979 (V1)		12/1978 to 12/1979 (V1)
NOAA-6/MSU	07/1979 to 03/1983 (V1) 05/1985 to 08/1986 (V1)	01/1981 to 03/1983 (V1) 11/1985 to 10/1986 (V1)	07/1979 to 02/1983 (V1) 11/1985 to 08/1986 (V1)
NOAA-7/MSU	09/1981 to 01/1985 (V1)	09/1981 to 01/1985 (V1)	08/1981 to 02/1985 (V1)
NOAA-8/MSU	05/1983 to 05/1984 (V1)	05/1983 to 08/1985 (V1)	05/1983 to 10/1985 (V1)

NOAA-9/MSU	03/1985 to 02/1987 (V1)	02/1985 to 02/1987 (V1)	03/1985 to 11/1988 (V1)
NOAA-10/MSU	12/1986 to 08/1991 (V2)	12/1986 to 08/1991 (V1)	11/1986 to 09/1991 (V1)
NOAA-11/MSU	12/1988 to 09/1994 (V2)	11/1988 to 04/1998 (V1)	11/1988 to 12/1998 (V1)
NOAA-12/MSU	10/1991 to 10/1998 (V2)	9/1991 to 11/1998 (V1)	09/1991 to 12/1998 (V1)
NOAA-14/MSU	01/1995 to 12/2004 (V2)	01/1995 to 9/2006 (V1)	04/1995 to 12/2004 (V1)
NOAA-15/AMSU-A	11/1998 to 12/2017 (V2)	11/1998 to 12/2010 (V1)	11/1998 to 12/2017 (V2)
NOAA-18/AMSU-A	01/2007 to 09/2015 (V2)	01/2007 to 09/2015 (V1)	06/2005 to 12/2014 (V2)
NOAA-19/AMSU-A	03/2009 to 06/2018 (OP)	03/2009 to 06/2018 (OP)	03/2009 to 12/2017 (OP)
MetOp-A/AMSU-A	01/2008 to 12/2017 (V2)	N/A (Channel failed since *12/16/2008*)	01/2008 to 12/2017 (V2)
Aqua/AMSU-A	08/2002 to 12/2009 (V1)	08/2002 to 12/2019 (V1)	08/2002 to 12/2009 (V1)
SNPP/ATMS	01/2012 to present (RP)	01/2012 to present (RP)	01/2012 to present (RP)
NOAA-20/ATMS	01/2018 to present (RP)	01/2018 to present (RP)	01/2018 to present (RP)

Other primary sensor data needed were warm target temperatures, geo-location information, and sensor quality flags that are also in orbital swath format.

3.3.2 Ancillary Data

The algorithm requires a set of ancillary data which will be provided in the delivery package.

i. Land-sea mask, 2.5^0x2.5^0 latitude/longitude grid resolution [A grid cell is considered as ocean (land) if the ocean percentage in the grid cell is greater (smaller) than 50%]

ii. Limb-adjustment dataset for adjusting AMSU-A observations made at different viewing angles to nadir views (Available in the system package for generation of MLT CDR)

iii. Limb-adjustment dataset for adjusting ATMS observations made at different viewing angles to nadir views (Available in the system package for generation of MLT CDR)

iv. Frequency adjustment dataset for adjusting MSU observations at different channel frequencies to match with the AMSU-A temperatures (Available in the system package for generation of MLT CDR)

3.3.3 Derived Data

The derived data is the Mean Layer Temperature - NOAA CDR v5.0. The CDR includes atmospheric layer temperatures of the lower-troposphere (TLT, roughly peaking at 3 km), mid-troposphere (TMT, roughly peaking at 5 km), upper-troposphere (TUT, roughly peaking at 10 km), and lower-stratosphere (TLS, roughly peaking at 17 km). The CDR is a monthly global dataset with 2.5^0x2.5^0 latitude/longitude grid resolution covering the period from late 1978 to present. The CDR merged microwave sounder observations from 16 polar-orbiting satellites including NOAA Polar-orbiting Operational Environmental Satellite (POES) series (TIROS-N to NOAA-19), MetOp-A, Aqua, and NOAA Joint Polar Satellite System (JPSS) series (SNPP and NOAA-20). Three generations of satellite microwave sounders were used in the CDR development, containing Microwave Sounding Unit (MSU) during 1979-2004, Advanced Microwave Sounding Unit-A (AMSU-A) during 1998-2017, and Advanced Technology Microwave Sounder (ATMS) from 2012 to present. The merging algorithm will be described in detail in Section 3.4. Table 2-1 summarizes data products derived from the input data.

3.3.4 Forward Models

The Community Radiative Transfer Model (CRTM) [*Han et al.*, 2006] was extensively used for deriving simulated AMSU-A limb-adjustment and frequency adjustment at each scan positions for corresponding satellite channels. The CRTM model is publicly available through NOAA/Joint Center for Satellite Data Assimilation (https://www.jcsda.org/jcsda-project-community-radiative-transfer-model). The NASA MERRA2 reanalysis data were used as input to the CRTM in all simulations. Two types of MERRA2 data, both with a spatial resolution of 0.5° latitude × 0.625° longitude, were used in the simulation: the hourly surface data containing skin temperature and wind vector and 3-hourly atmospheric profiles including temperature, water vapor, ozone, cloud liquid water, and wind vector. These data were interpolated into those of satellite time and locations for each scan positions for the CRTM to generate simulated correction time series at corresponding swath time and geo-location for each satellite channels.

3.4 Theoretical Description

This section reviews various bias correction algorithms for developing merged MSU/AMSU-A/ATMS MLT TCDR.

3.4.1 Physical and Mathematical Description

Development of MLT CDR involved bias correction for several different sources of error. These included incident angle effect, calibration drift, diurnal sampling drift, solar-

heating induced warm target effect on observed brightness temperature, and frequency differences between MSU and AMSU-A companion channels. Bias correction and merging algorithms used for developing the Mean Layer Temperature - NOAA CDR v5.0 was described in detail in Zou et al. (2023). These algorithms are briefly described in the following subsections.

3.4.1.1 Recalibration of MSU and AMSU-A Observations

The Mean Layer Temperature - NOAA CDR v5.0 used recalibrated BTs as inputs for selected MSU and AMSU-A channels. The purpose of recalibration was to remove drifting errors found in pre-launch operational calibration. The level-1 recalibration algorithm uses cold space views and internal blackbody warm target views to calibrate scene temperatures from the Earth views. The recalibration algorithm was described in detail in Appendix A in Zou et al. (2023) and it is written as

$$R_e = R_L - \delta R + \mu Z \tag{3.1}$$

where R_e is the earth scene radiance, $R_L = R_c + G^{-1}(C_e - C_c)$, representing the dominant linear response, and $Z = G^{-2}(C_e - C_c)(C_e - C_w)$ is a quadratic nonlinear response characterizing the non-perfect square law nature of a detector. C represents the raw counts value of the satellite observations and $G = \frac{(C_w - C_c)}{(R_w - R_c)}$ is the instrument gain. The subscripts *e, w* and *c* refer to the earth-view, onboard blackbody warm target view, and cold space view, respectively; and δR and μ are calibration coefficients.

Eq. (3.1) is modified version of the calibration equation used in NOAA operational calibration (e.g., Mo 1995, 1996). In pre-launch operational calibration, calibration coefficients in the calibration equation were obtained from thermal-vacuum chamber test data. In the post-launch recalibration as used in Mean Layer Temperature - NOAA CDR v5.0, however, calibration coefficients were assumed to vary linearly over time, i.e.,

$$-\delta R = \delta R_0 + \kappa(t - t_0) \tag{3.2}$$

$$\mu = \mu_0 + \lambda(t - t_1) \tag{3.3}$$

here t is time, t_0 and t_1 are reference times, and δR_0, κ, μ_0, *and* λ are calibration coefficients. These coefficients were obtained from SNO regressions in post-launch recalibration (Zou et al. 2023).

Three possible mechanisms were proposed in Zou et al. (2023) to explain calibration drifts: i) time-varying side-lobe effect resulting from possible degradation in reflector or antenna materials; ii) possible change over time in the blackbody warm target emissivity. The blackbody temperature is measured by the platinum resistance thermometers (PRTs) embedded in the blackbody target, but a degradation in blackbody emissivity could cause a bias drift in the blackbody radiometric temperature; iii) degradation in detector or amplifier may cause changes in calibration nonlinearity, which causes calibration bias drift as well as solar-heating related seasonal variability in TB.

There are two sets of calibration coefficients corresponding two versions of recalibrated BT FCDRs. Table 3-1 and Table 3-3 listed Version 1 (V1) calibration coefficients for V1 MSU FCDR and V1 AMSU-A FCDR, respectively. These coefficients were obtained in Zou et al. (2006, 2009, 2010) for MSU and Zou and Wang (2011) for AMSU-A. Table 3-2 and Table 3-4 listed Version 2 (V2) calibration coefficients for V2 MSU FCDR and V2 AMSU-A FCDR, respectively. These coefficients were obtained in (Zou et al. 2023). Version 2 calibration coefficients removed calibration drifts for selected MSU/AMSU-A channels based on new reference observations that were unavailable during the development of V1 calibration coefficients. As a demonstration in Figure 3-5a, the NOAA-15 AMSU-A channel 5 observations showed a cooling drift relative to the same channel observations onboard MetOp-A during 2007-2017 and a solar-heating induced TB variability after 2015. Recalibration by Zou et al. (2023) using the V2 calibration coefficients had successfully removed the cooling drift and reduced the TB variability. In addition, the V2 recalibration coefficients also removed spurious warming drifts in the MSU channel 2 observations onboard NOAA-11 through NOAA-14 (Figure 3-5b). This made the observations in NOAA-11 through NOAA-14 consistent with the reference observations as described in Section 3.4.1.3.

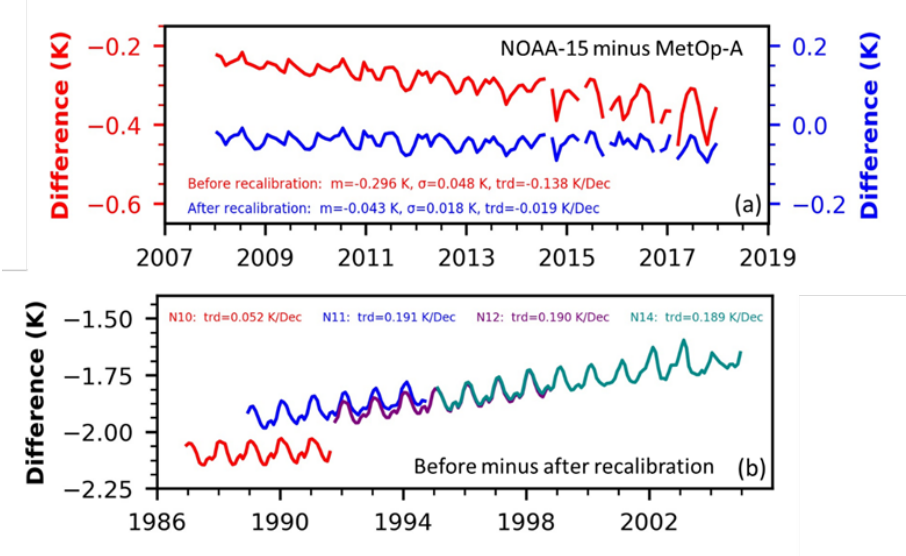

Figure 3-5. a) Inter-satellite difference time series of global ocean mean brightness temperatures of AMSU-A channel 5 between NOAA-15 and MetOp-A, for before and after recalibration. b) Global mean difference time series for before minus after recalibration for MSU channel 2 observations onboard NOAA-10 through NOAA-14. Plots were from Zou et al. (2023).

3.4.1.2 Limb Adjustment

A limb-adjustment adjusts radiances at off-nadir viewing angles to those close to the nadir direction. This adjustment is necessary for use of the off-nadir footprints in the time series to increase observational samples and reduce noise and sampling-related biases.

Different limb-adjustment approaches were applied for the MSU and AMSU-A instruments, respectively. Limb-adjustment algorithms and coefficients for the MSU observations had been developed by Goldberg et al. (2001) using statistical methods. Zou et al. (2009) examined the impact of the limb-adjustment on the MSU time series and found robust trend results when different limb-adjusted footprints were included in the time series. In developing NOAA MSU Level-1c radiance FCDR datasets, limb-adjustment based on Goldberg et al. (2001) approach was applied to the IMICA calibrated radiances for each scan positions. These limb-adjusted radiances were saved in the corresponding MSU Level-1c orbital files which were directly extracted and used in the generation of gridded MSU temperatures. Therefore, limb-adjustment for MSU was not part of the merging algorithms as provided in the software package.

Limb-adjustment for the AMSU-A observations was based on CRTM simulations developed in Wang and Zou (2014). In this approach, the limb-adjustment was the CRTM simulated differences for each scan position between those with off-nadir and zero scan angles. The simulations were conducted for each satellite to accommodate their different altitudes and scan positions. The NASA's Modern-Era Retrospective analysis for Research and Applications, Version 2 (MERRA2, Gelaro et al. 2017) reanalysis was used as inputs to the simulation. Off-nadir biases can be as large as more than 10 K, depending on scan angles, before limb-adjustment (Goldberg et al. 2001, Wang and Zou 2014). They were reduced to less than 0.1 K for scan positions 8-23 for most channels after the limb-adjustment (Wang and Zou 2014, Figure 3-6a). Limb adjustments to the ATMS data were based on limb correction coefficients developed by Zhang et al. (2017). This adjustment resulted in off-nadir biases within 0.2 K for all off nadir footprints (Figure 3-6b).

After the limb-adjustment, monthly gridded data were generated, for ascending and descending orbits separately, by accumulating and binning limb-adjusted brightness temperature into grid cells with a resolution of 2.5° latitude by 2.5° longitude and then averaged in monthly intervals. Each MSU scanline contains 11 fields of view (FOVs); limb-adjusted views from the scan positions 3 to 9 were used in the monthly grid cells. Similarly, each AMSU-A scanline has 30 FOVs. Among them, limb-adjusted views from the scan positions 8 to 23 were used in the monthly gridded products to match with the MSU swath width. Of the 96 footprints in an ATMS scan line, the near-nadir footprints from scan positions 29 to 68 were used to match with the swath width of MSU and AMSU-A.

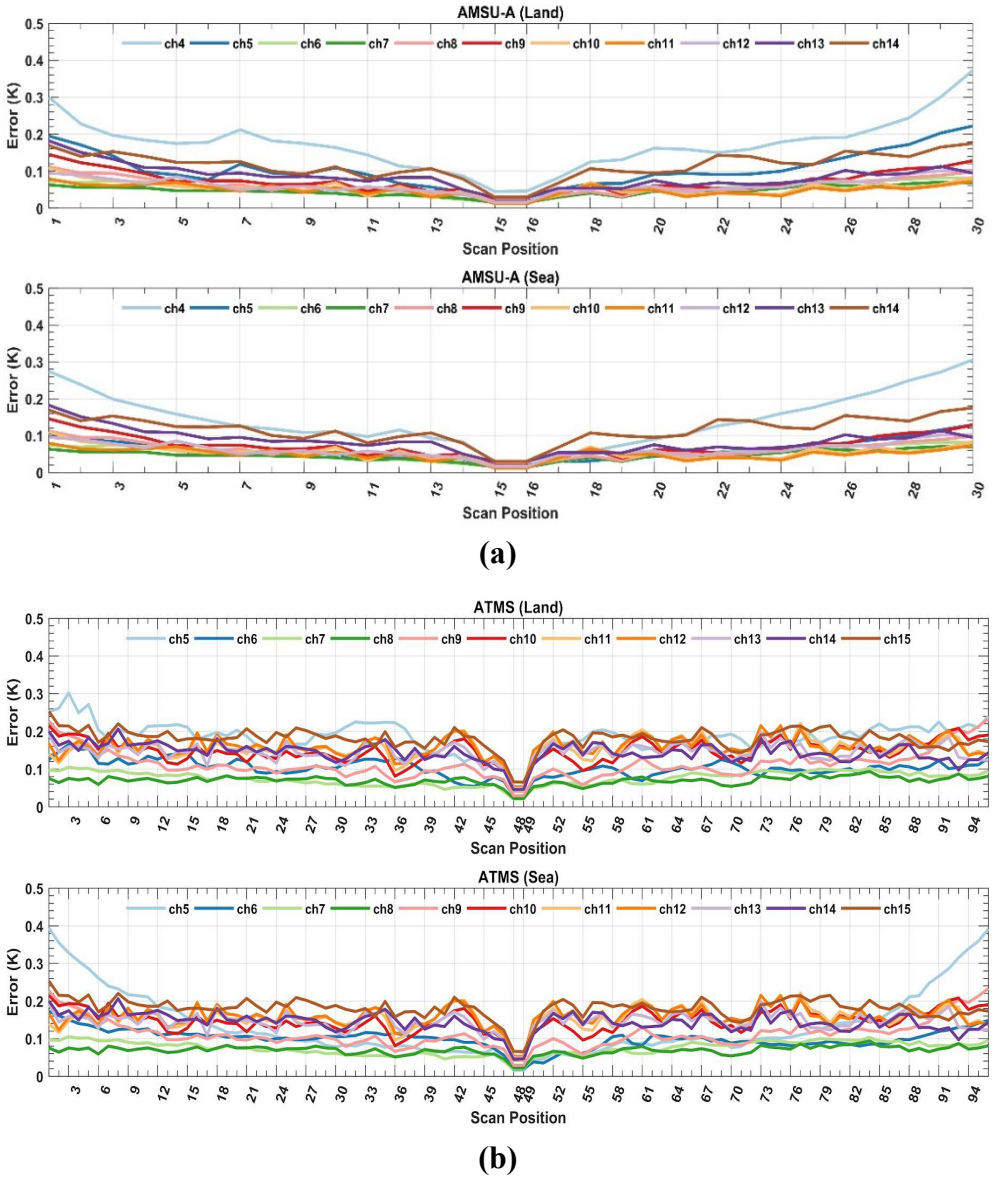

Figure 3-6. (a) Off nadir biases after limb-adjustment for a) AMSU-A channels 4-14 for all scan positions and b) ATMS channels 5-15 for all scan positions. Land and ocean are plotted separately.

3.4.1.3 Reference Time Series

A unique feature in Mean Layer Temperature - NOAA CDR v5.0 is it relies on a reference time series to inter-calibrate satellite data records with a backward merging approach. The satellites for developing the reference time series include Aqua, MetOp-A, SNPP, and NOAA-20. These satellites are all in stable sun-synchronous orbits (Figure 1-1b), as such, diurnal drift adjustment is not needed. In addition, these satellites had achieved high radiometric stability

performance (Zou et al. 2018), allowing their merged time series to have high accuracy in trend detection (Zou et al. 2021).

The procedure to construct the reference time series from the satellites in stable orbits has been described in Zou et al. (2021). Following this procedure, the deseasonalized BT anomalies are first calculated, which are defined as BT minus its monthly climatology for the ascending and descending orbits for each satellite and for each grid point. Here the monthly climatology was calculated from the entire observation periods for each satellite. Figure 3-7 shows the global mean anomaly difference time series for TMT, TUT, and TLS, respectively, between ascending and descending orbits for the four satellites. The means of the anomaly differences are exactly zero by their definition, with a standard deviation of 0.007–0.012 K. The trends of anomaly differences are less than 0.02 K/Decade (0.002 K/year) that are statistically insignificant for all satellites.

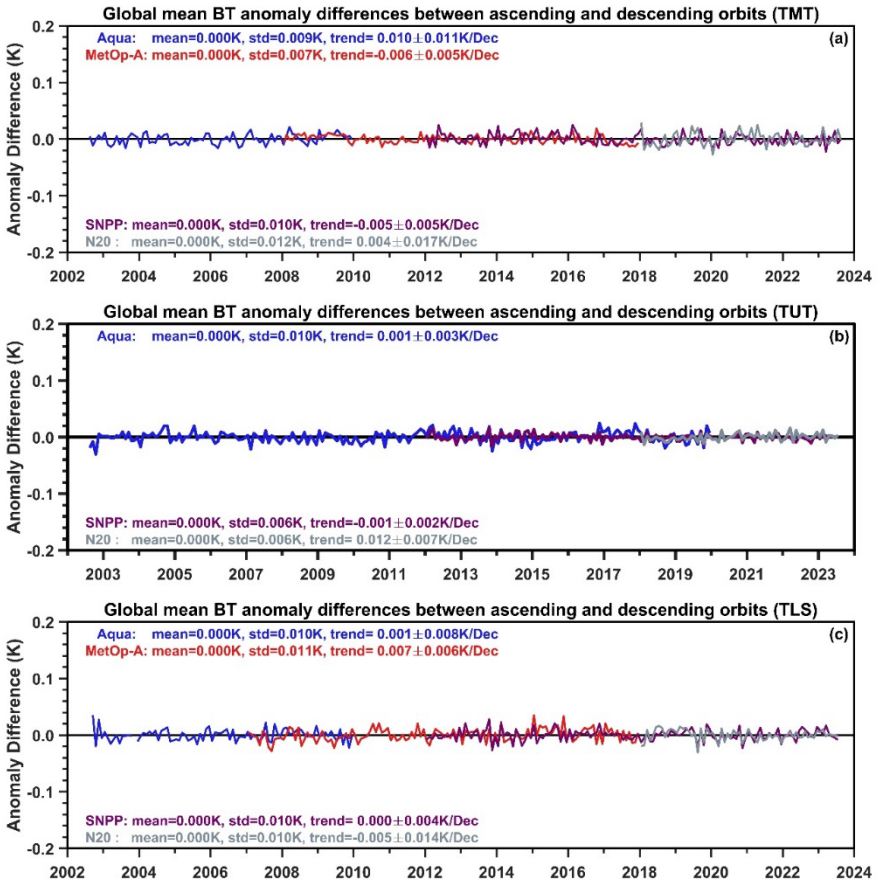

Figure 3-7. Global mean BT anomaly differences between ascending and descending orbits. The differences are for ascending minus descending (1:30 p.m. minus 1:30 a.m.) for Aqua (blue), SNPP (purple) and NOAA-20 (gray), and descending minus ascending (9:30 a.m. minus 9:30 p.m.) for MetOp-A (red). The anomalies are relative to the monthly climatology calculated for the entire observation periods for each satellite; a) TMT channels; b) TUT channels; c) TLS channels.

With little differences, the ascending and descending anomalies were averaged to give the daily mean anomalies for each satellite. To merge the BT anomalies from different satellites, an adjustment is needed so that the BT anomalies of individual satellites are defined relative to the same monthly climatology. For TMT, the MetOp-A monthly climatology was used as a reference and then Aqua and SNPP anomalies were adjusted by subtracting a "monthly climatology" of the anomaly differences relative to MetOp-A during their overlapping periods. NOAA-20 was then adjusted to the adjusted SNPP using their overlaps. After this adjustment, the anomalies from the four satellites are merged together to generate a reference TMT (RTMT) time series for the entire period from 2002 to present. Similar procedure is used for developing RTUT and RTLS, except that the SNPP observations were used as a reference in the climatology adjustment. Figure 3-8 shows the merged anomaly time series for RTMT, RTUT, and RTLS, as well as inter-satellite difference time series before their merging.

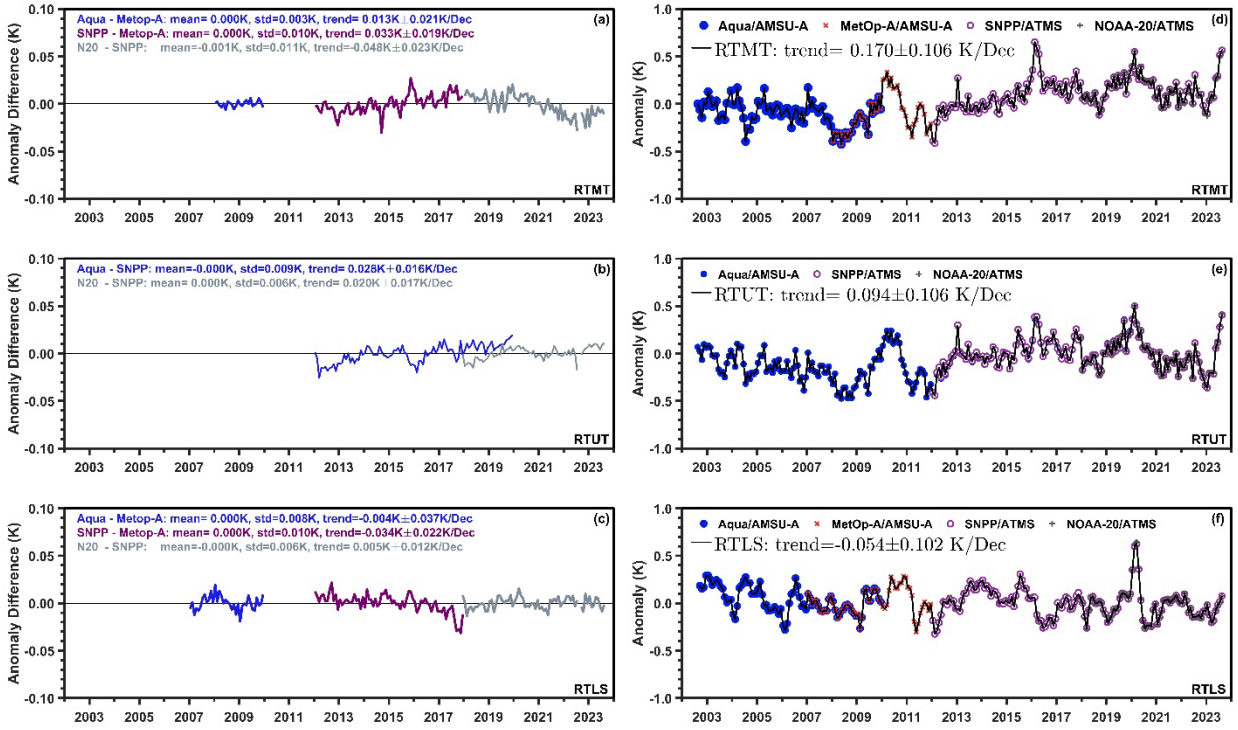

Figure 3-8. Monthly global mean BT anomaly time series for Aqua, MetOp-A, SNPP, and NOAA-20 and the reference time series merged from these satellites (right panels). a) Inter-satellite difference time series before merging for RTMT; b) Inter-satellite difference time series before merging for TUT; c) Inter-satellite difference time series before merging for TLS; d) RTMT and individual anomaly satellite time series; e) RTUT and individual anomaly satellite time series; and f) RTLS and individual anomaly satellite time series. Anomalies are relative to a monthly climatology of the MetOp-A period from January 2008 to December 2017 for RTMT, and to a climatology of the SNPP period from January 2012 to December 2022 for RTUT and RTLS. Uncertainties in trend calculations represent 95% confidence intervals with autocorrelation adjustments.

When used as a reference in satellite merging, the monthly climatology averaged from ascending and descending orbits from the reference satellite was added to the reference MLT anomalies in order to recover the absolute values of the brightness temperature at each grid point. For RTMT, the reference was MetOp-A during 01/2008-12/2017. For RTUT and RTLS, the reference was SNPP during 01/2012-12/2022. Note that a monthly climatology from ascending or descending only orbits is defined at the ascending or descending local times, while their averages give the recovered reference MLT as a monthly mean 'daily' time series which is not associated with a specific local time.

3.4.1.4 Frequency Adjustment for MSU Observations

Due to differences in channel frequencies, the MSU channels and AMSU-A channels have slightly different weighting functions and thus measure different layers of the atmosphere at the nadir direction (Figure 2-1). This results in scene temperature differences because the atmospheric temperature has a non-zero lapse rate. The varying atmospheric lapse rates over time and space would cause the scene temperature differences to vary over time and geolocation. Figure 3-9 shows inter-satellite difference time series before frequency adjustment for different channels. The differences between NOAA-14 MSU channel 2 and NOAA-15 AMSU-A channel 5 are particularly large (Figure 3-9a) owing to their channel frequency differences and large lapse rate in the mid-troposphere. These differences must be removed for the two instrument observations to be merged together for CDR development.

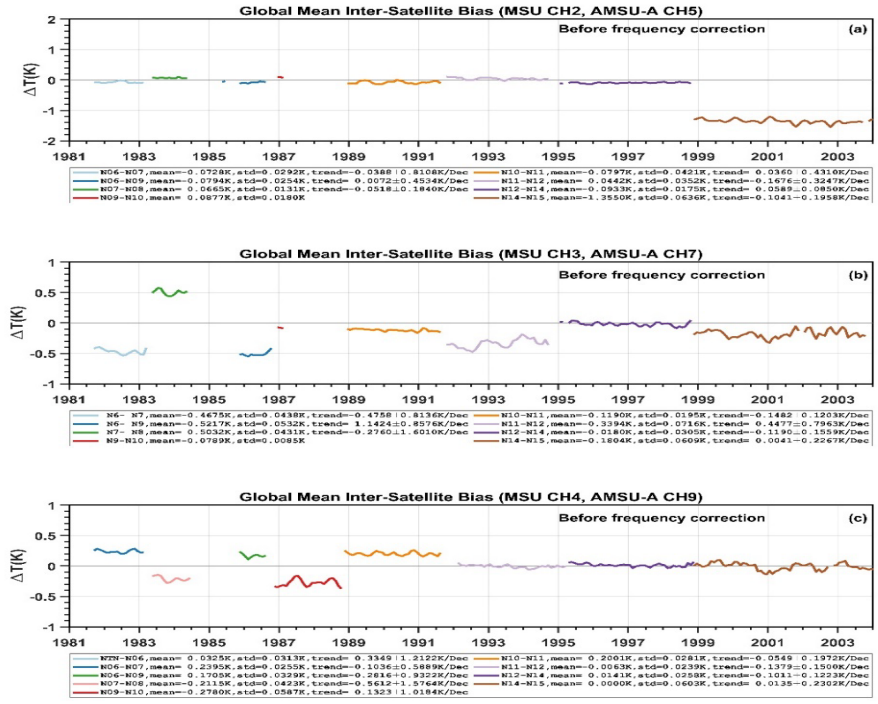

Figure 3-9. Monthly global mean BT difference time series before MSU frequency adjustment. a) MSU channel 2; b) MSU channel 3; and c) MSU channel 4.

The frequency adjustment in the STAR MLT CDR included two steps. The first was to derive a first-guess adjustment based on CRTM simulations. Here in two simulations, the CRTM setups were exactly the same except the channel frequency inputs were taken from the AMSU-A channels and MSU channels, respectively. The frequency adjustment was taken as the simulated TB differences between the two simulations using NASA MERRA2 reanalysis as inputs. Two types of MERRA2 data, both with a spatial resolution of 0.5^0 latitude × 0.625^0 longitude, were used in the simulation: the hourly surface data containing skin temperature and wind vector and 3-hourly atmospheric profiles including temperature, water vapor, ozone, cloud liquid water, and wind vector. The simulation was conducted for six-year MERRA2 data (1998.11-2004.12) during which NOAA-14 overlapped with NOAA-15. This simulation was then converted to a $2.5^0 \times 2.5^0$ gridded monthly climatology for frequency adjustment of all satellites from NOAA-14 to TIROS-N. Figure 3-10 shows an example of the CRTM simulated frequency adjustment for January for the TMT product. Figure 3-11a shows actual differences between the MSU channel 2 and AMSU-A channel 5 observations before frequency adjustment. After the first-guest adjustment, differences between the MSU and AMSU-A were largely reduced but they were still non-zero owing to residual calibration errors over the ocean and diurnal differences over land (Figure 3-11b).

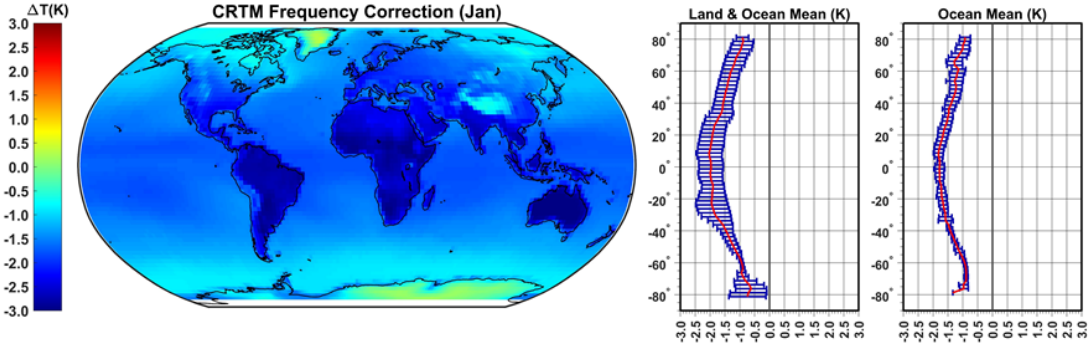

Figure 3-10. CRTM simulated frequency adjustment term for January TMT product between MSU channel 2 and AMSU-A channel 5 (MSU Ch2 minus AMSU-A Ch5). The left panel is the global distribution and the right panels are latitudinal means for land plus ocean and ocean only, respectively.

To remove possible calibration errors and as a second step, the first-guess adjustment was modified by a climatology derived from the differences between NOAA-15 and NOAA-14 over the ocean. This climatology was calculated by averaging the NOAA-15 and NOAA-14 differences for the same month at each grid point through the period from January 1999 to December 2004. These gridded differences were further averaged in latitudinal belts over the ocean to derive a zonal mean climatology which was used to modify and constrain the zonal mean magnitude of the first-guess adjustment so that the latter quantity equals the former for each month and latitude. In this way, the final frequency adjustment term equals the latitudinal climatology over the ocean while adjustments at individual grid points follow lapse rate structures from the CRTM simulations. Figure 3-11c shows effects after the climatology adjustment for MSU channel 2 and AMSU-A channel 5. For TMT product, the frequency adjustment for the NOAA-14 MSU channel 2 and

NOAA-15 AMSU-A channel 5 was applied to all other MSU satellites from TIROS-N to NOAA-12.

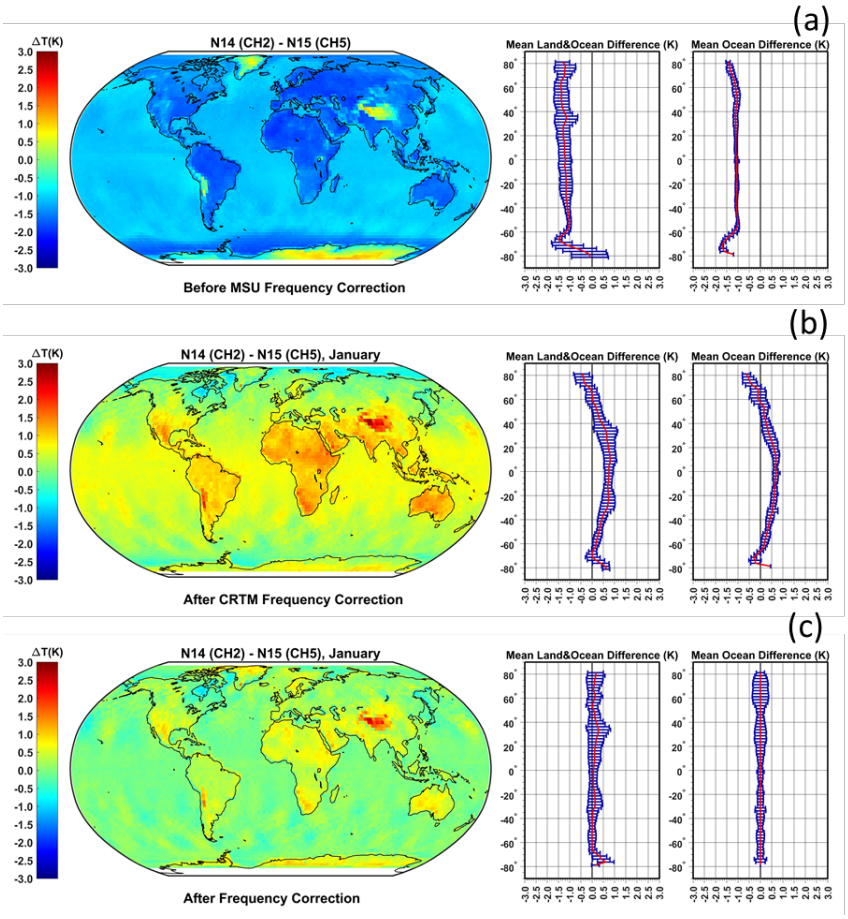

Figure 3-11. Impact of frequency adjustment on the differences in January between MSU channel 2 and AMSU-A channel 2. a) Observed differences before frequency adjustment; b) Differences after the CRTM-simulated frequency adjustment; c) Differences after the climatology adjustment. The left panel is the global distribution and the right panels are latitudinal means for land plus ocean and ocean only, respectively.

For the MSU channel 3, post-launch frequency shift was found for most MSU satellites (Lu and Bell 2014). As a result, the first step CRTM adjustment plus the second step climatology adjustment using NOAA-14 MSU and NOAA-15 AMSU-A differences are insufficient to remove inter-satellite biases for other MSU pairs. As such, a successive residual bias correction was applied to other MSU satellites using climatology. This successive procedure started from the corrected NOAA-14 MSU channel 3 backward all the way to NOAA-6. In specific, after NOAA-14 was adjusted to NOAA-15, NOAA-12 was then adjusted to the adjusted NOAA-14, NOAA-11 was then adjusted to the adjusted NOAA-12, and so on following the order illustrated in Figure 3-12.

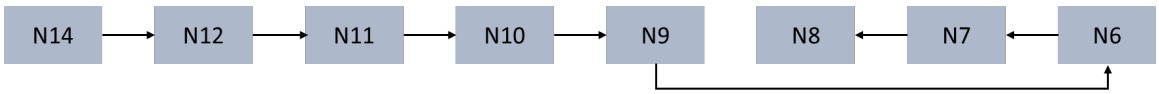

Figure 3-12. Successive residual bias correction for frequency differences for MSU satellites using climatology.

Figure 3-13 and Figure 3-14 show inter-satellite biases for the MSU channel 3 before and after the frequency adjustments. As shown, inter-satellite biases are small for all satellite pairs with zero zonal means after the frequency adjustment.

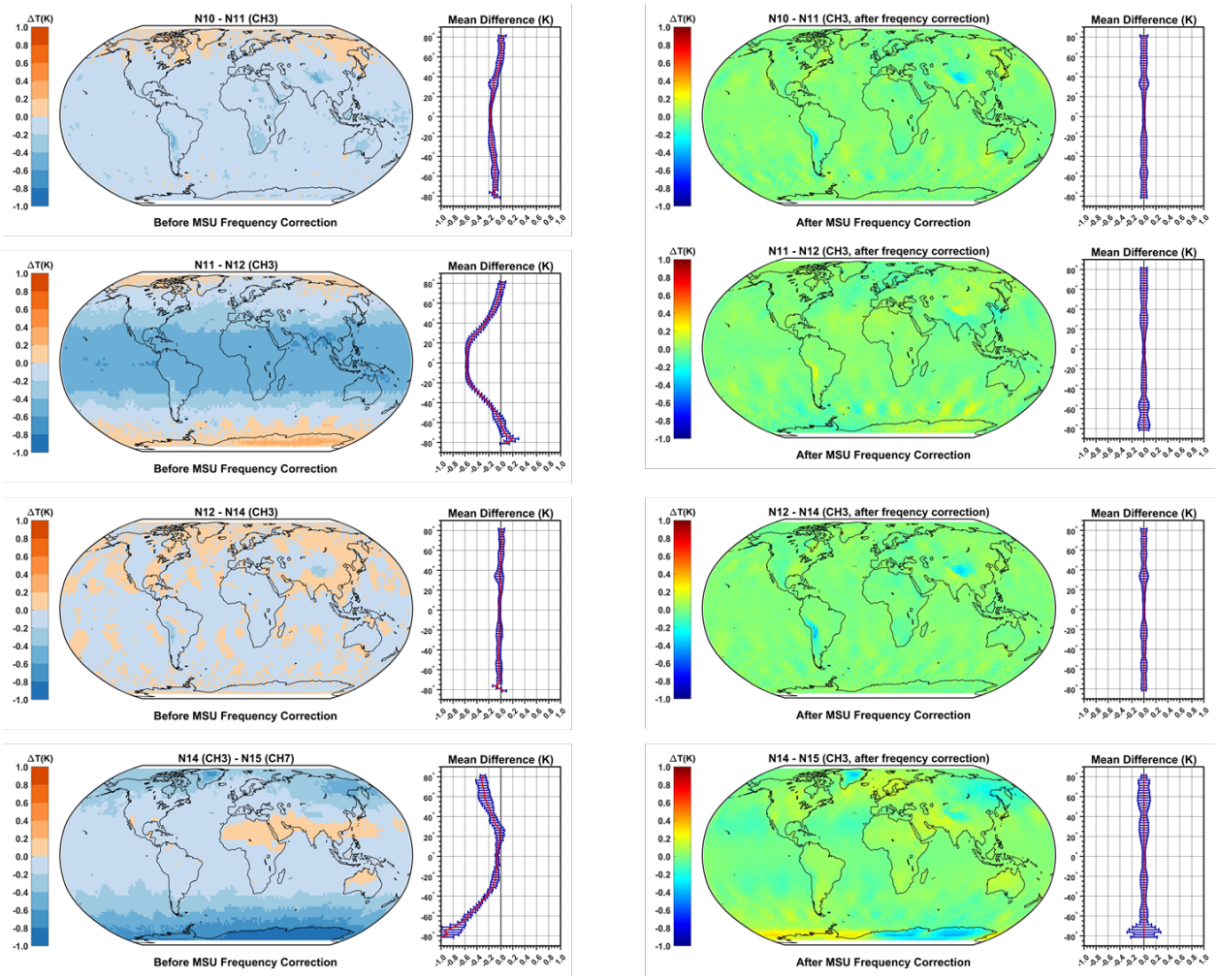

Figure 3-13. Impact of frequency adjustment on the differences in January between different MSU satellites (NOAA-10 to NOAA-14, upper three panels) and between MSU channel 3 and AMSU-A channel 7 (lower panels). Left panels are observed differences for the global distribution and latitudinal means before frequency adjustment. The right panels are similar difference maps but after the frequency adjustment.

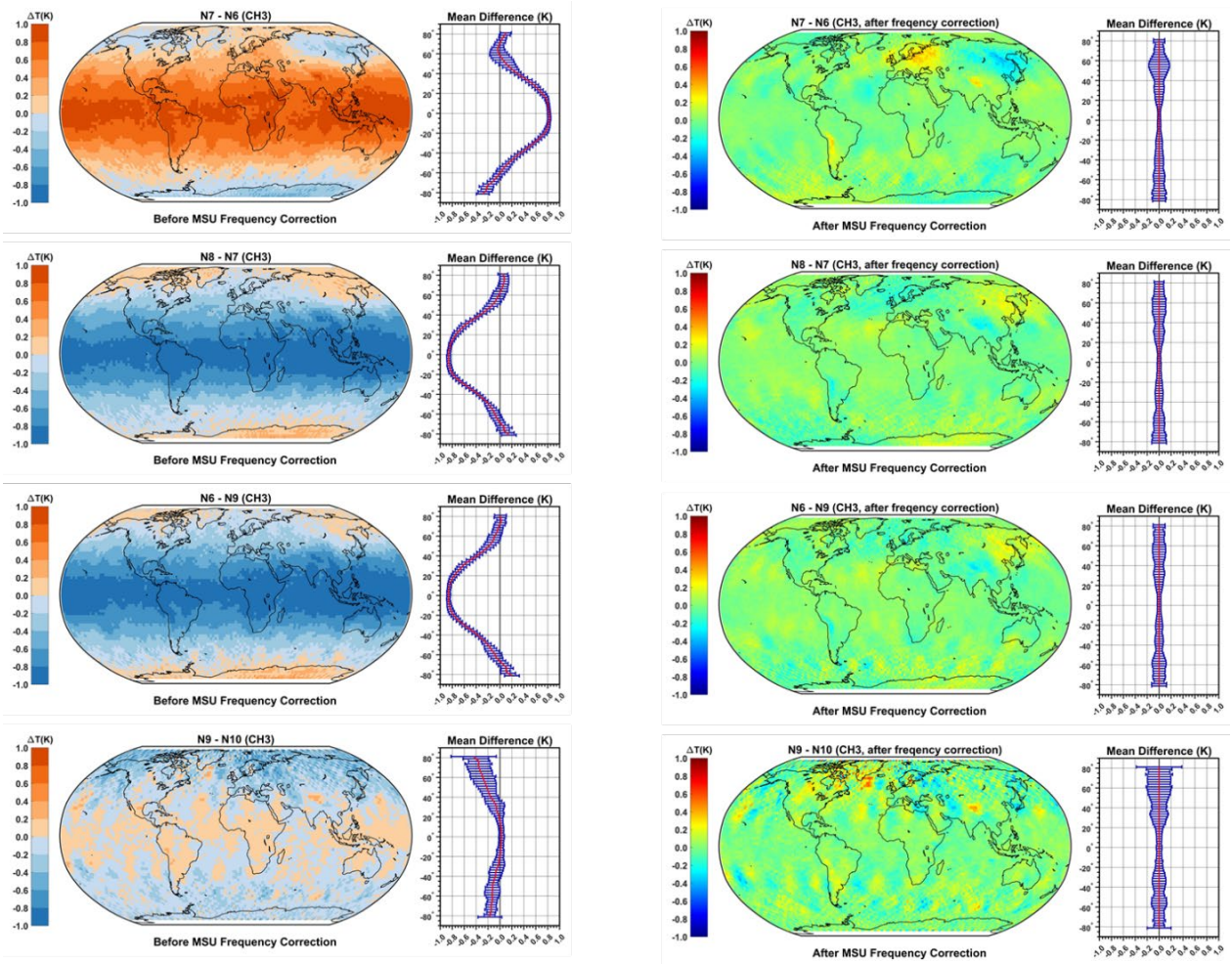

Figure 3-14. Impact of frequency adjustment on the differences in January between MSU satellite pairs from NOAA-6 to NOAA-10. Left panels are observed differences for the global distribution and latitudinal means before frequency adjustment. The right panels are similar differences but after the frequency adjustment.

3.4.1.5 Diurnal Drift Correction

The diurnal drift effect is caused by satellite orbital drift that results in changes in local observation time. Biases caused by diurnal drift can be removed by adjusting the scene brightness temperatures at different observation time from all different satellites to a common local time before satellite merging.

The diurnal cycle used for such an adjustment is a function of time and geolocation. In Mean Layer Temperature - NOAA CDR v5.0, an innovative semi-physical

diurnal model was developed to remove diurnal drifting errors with satellites from TIROS-N through NOAA-19 (Figure 1-1b). The diurnal model assumed that diurnal temperature changes are sine and cosine functions of the satellite local equator crossing time (LECT, Figure 1-1b), with both diurnal and semi-diurnal components being included in the sine and cosine functions. This is mathematically written as

$$D_j\left(\boldsymbol{X}, m, L_j\right) = a_j(\boldsymbol{X}) + \sum_{i=1}^{2}[\, b_i(\boldsymbol{X}, m)\, sin\left(i\omega L_j\right) + c_i(\boldsymbol{X}, m)\, cos\left(i\omega L_j\right)], \tag{3.4}$$

where D_j is the diurnal anomaly for satellite j at the geolocation $\boldsymbol{X}$, month m, and local overpassing time L_j, here L_j is a function of year t and month m; $\omega=2\pi/24$, the frequency of diurnal cycle, and $b_i(\boldsymbol{X}, m)$ and $c_i(\boldsymbol{X}, m)$ are periodic functions characterizing the amplitudes of the monthly diurnal and semi-diurnal components with a period of 1 year (i.e., both $b_i(\boldsymbol{X}, m)$ and $c_i(\boldsymbol{X}, m)$, $i=1,2$, contains 12 coefficients representing 12 months at geolocation $\boldsymbol{X}$). Here the coefficients $b_i(\boldsymbol{X}, m)$ and $c_i(\boldsymbol{X}, m)$ are assumed the same for different satellites but different for ascending and descending nodes and different instrument types (MSU and ANSU-A). The coefficient $a_j(\boldsymbol{X})$ is a combination of fitting coefficient and the yearly mean difference between satellite j and the reference satellite.

Actual diurnal air temperatures vary follow a quasi-sinusoidal pattern during daytime and a thermal decay process during nighttime. As such, the diurnal model is physically-based during daytime but an empirical model during nighttime. As such, the model is referred to as a semi-physical diurnal model. The model parameters $a_j(\boldsymbol{X})$, $b_i(\boldsymbol{X}, m)$ and $c_i(\boldsymbol{X}, m)$ were resolved using regressions of satellite overlapping observations. The key part is to solve the satellite ascending and descending diurnal cycles separately to account for different physical processes during daytime and nighttime. Figure 3-15 shows inter-satellite difference time series ($\Delta TB_{jk}=TB_j - TB_k$) for TMT, compared with diurnal cycle differences ($\Delta D_{jk}=D_j-D_k$) obtained from the semi-physical model for all satellite pairs from TIROS-N to the reference time series, land and ocean and ascending and descending orbits separately. Figure 3-16 shows impact of the diurnal drift adjustment on inter-satellite difference time series. As seen, diurnal drift adjustment with the diurnal model nicely removed diurnal drifting errors and resulted in inter-consistent observations between the reference and earlier satellites with orbital drifts.

Diurnal adjustment was not conducted for TLS since its diurnal amplitude is small. Diurnal adjustment for TUT was performed, but since its diurnal amplitude was also small and thus not shown here.

A more detailed description of the model development and its performance discussion can be found in Zou et al. (2023).

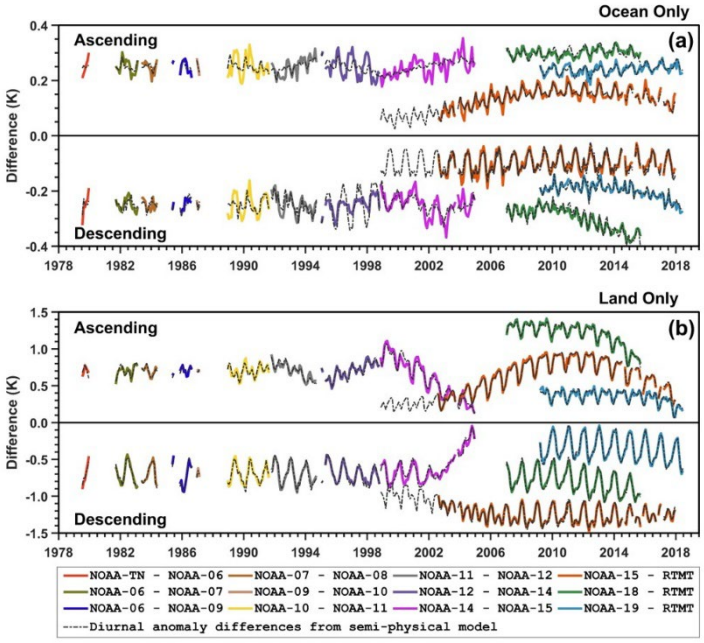

Figure 3-15. Inter-satellite differences for TMT (ΔTBjk = TBj− TBk, colored solid lines) and diurnal anomaly differences (ΔDjk = Dj− Dk, dashed lines) derived from the semi-physical model for (a) over the global ocean and (b) over the global land. Differences were grouped into ascending and descending data separately by adding constant offsets to different satellite pairs for an adjustment. As such, the vertical temperature coordinate does not necessarily represent the actual values or signs of the mean diurnal anomaly differences, but they represent the magnitudes of the seasonal cycle and drifting range of the diurnal anomaly differences. The NOAA-15 diurnal anomalies during the 3.5-year period from November 1998 to July 2002 were predicted from the semi-physical model based on regression coefficients obtained from its overlaps with RTMT during August 2002–December 2017. Plot is from Zou et al. (2023).

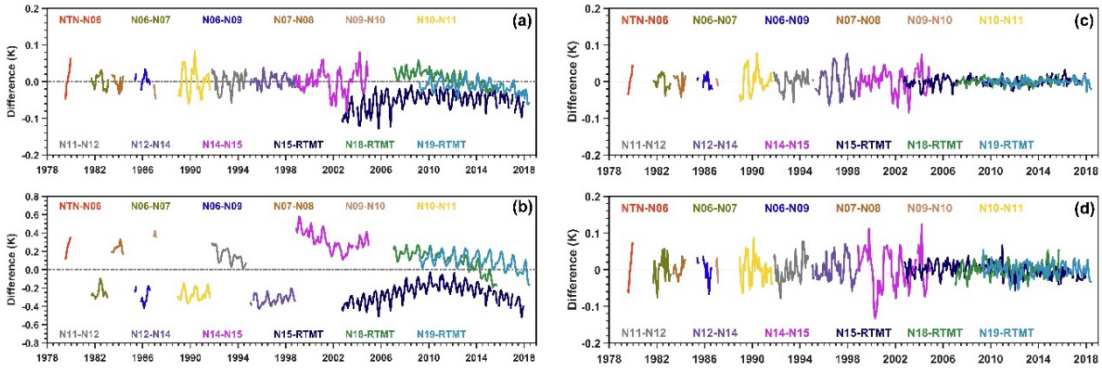

Figure 3-16. Impact of diurnal adjustment on the TMT inter-satellite differences. a) Inter-satellite difference time series over the global ocean for satellite pairs between those from TIROS-N to RTMT before adjustment; b) same as a) but over the global land; c) same as a) but for after diurnal adjustment; d) same as b) but for after diurnal adjustment. Plot is from Zou et al. (2023).

3.4.1.6 Instrument Temperature Variability in Radiances

A blackbody warm target was used to calibrate the MSU and AMSU-A raw counts observations to obtain level-1c radiances. The warm target temperature was measured by the Platinum Resistance Thermometers (PRTs) embedded in the blackbody. The blackbody target temperature exhibited large seasonal variability and long-term trends for most MSU satellites and NOAA-15 (Figure 3-17) due to solar-heating changes related to changes in solar β-angle (Zou and Wang 2011). These variability and trends were largely reduced by the level-1c recalibration with the SNO approach. However, small residual variability and biases still existed due to imperfect

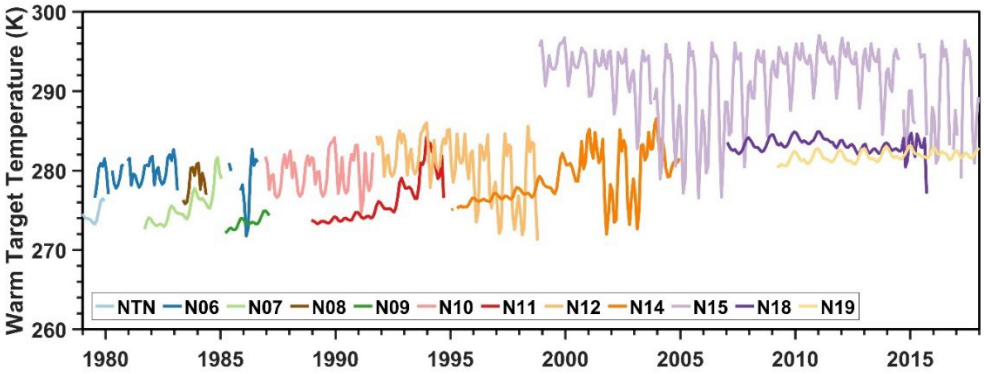

Figure 3-17. Global mean warm target time series of the NOAA satellite series from TIROS-N to NOAA-19.

calibration. These residual biases need to be removed before satellite merging. Here an empirical algorithm developed by Christy et al. (2000) is implemented to remove the radiance errors due to this warm target effect. This approach finds a best fitting empirical relationship between the correction term of the level-3 gridded brightness temperatures and warm target temperatures and then removes the best fit from the unadjusted time series. Using TB_a and TB_u to respectively represent adjusted and unadjusted brightness temperatures, this empirical approach can be mathematically expressed as

$$\mathrm{TB_a} = \mathrm{TB_u} - \beta - \alpha \mathrm{T'_w} \tag{3.5}$$

where $T_w^{'}$ denotes the warm target temperature anomaly, β a constant and α the warm target factor. These two parameters were resolved by regressions of satellite overlapping observations of the global ocean means after the diurnal drift adjustment was conducted. Table 3-6 lists the resulting warm target factors resolved from regressions for all satellites for TMT, TUT, and TLS. Figure 3-18 shows monthly global mean inter-satellite difference time series for all satellite pairs after adjustment of the warm target effect for TMT, TUT, and TLS. As seen, inter-satellite differences for each satellite pair were zero, the standard deviations of inter-satellite differences were

Table 3-6. Warm target factors (10^{-2}).

	NTN	N06	N07	N08	N09	N10	N11	N12	N14	N15	N18
TMT	1.55	-0.27	0.53	1.50	-0.47	-0.58	0.23	-0.45	0.77	0.15	-0.29
TUT		0.09	0.57	0.75	-0.42	-0.12	1.25	-0.02	-1.38	-0.36	
TLS	-0.40	0.22	-2.05	1.35	-2.56	1.04	-0.37	-0.01	0.99	0.04	0.82

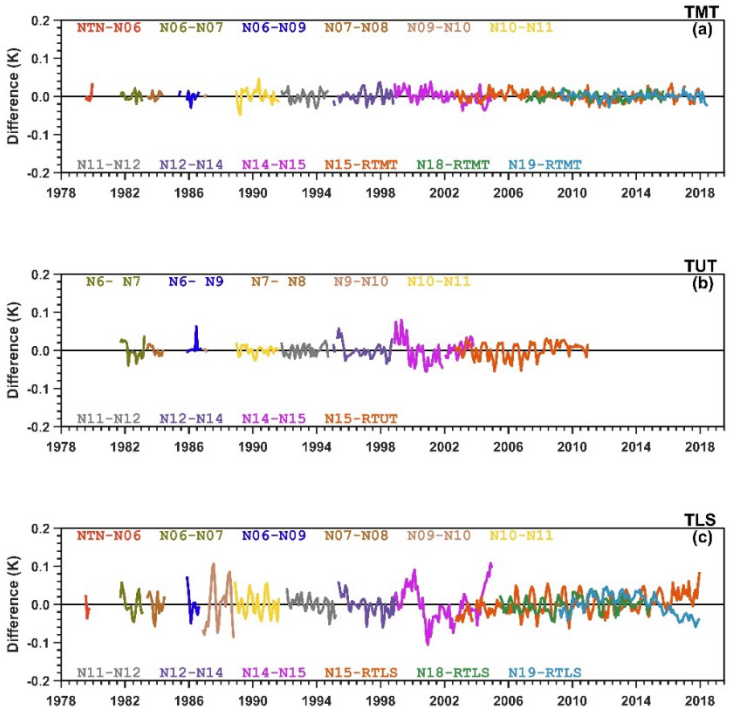

Figure 3-18. Inter-satellite difference time series for satellite pairs between those from TIROS-N to the references after all adjustments for (a) TMT, (b) TUT, and (c) TLS.

minimized, and trend differences between satellite pairs were close to zero. Observations from different satellites are ready to be merged together to generate single time series after this adjustment.

3.4.1.7 Derivation of TLT Time Series

The Mean Layer Temperature - NOAA CDR v5.0 TLT is derived using combinations of TMT, TUT, and TLS. It is calculated by the following formula: TLT=1.430×TMT-0.462×TUT+0.032×TLS. The regression coefficients (1.430, -0.462, 0.032) were obtained by fitting AMSU-A channel 4 weighting function using the TMT, TUT, and TLS weighting functions

with a slight adjustment so that the resulting TLT weighting function does not have negative values over the lower stratosphere. Figure 3-19 shows weighting functions for AMSU-A channel 4 (TLT, pink curve), TMT (AMSU-A channel 5), TUT (AMSU-A channel 7), TLS (AMSU-A channel 9), and the obtained Mean Layer Temperature - NOAA CDR v5.0 TLT (fitted TLT, thick black curve).

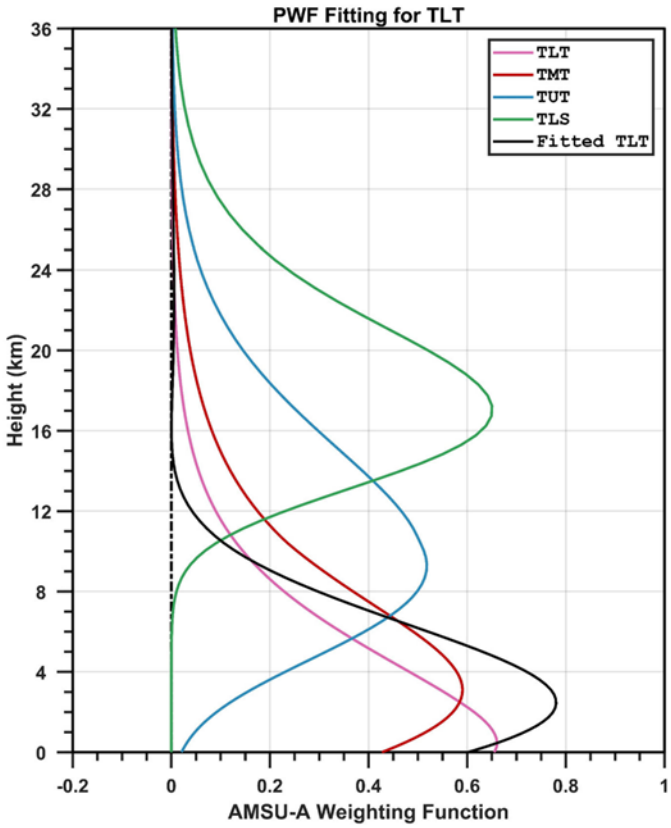

Figure 3-19. Weighting functions for AMSU-A channel 4 (TLT, pink curve), TMT (AMSU-A channel 5), TUT (AMSU-A channel 7), TLS (AMSU-A channel 9), Mean Layer Temperature - NOAA CDR v5.0 TLT (fitted TLT=1.430×TMT-0.462×TUT+0.032×TLS, thick black curve).

3.4.2 Data Merging Strategy

After applying the set of adjustments mentioned in the previous sections, the mean of the inter-satellite biases was numerically close to zero. The standard deviation of the inter-satellite biases was also significantly reduced compared with unadjusted data. As a result, the adjusted BT data from different spacecrafts and the references are treated as a homogenous CDR and then these observations were simply averaged on each grid cells to obtain a merged MLT CDR covering the period from late 1978 to present.

3.4.3 Numerical Strategy

Most of the bias adjustment procedures are straightforward in numerical calculations once the level-1c radiances are extracted from the MSU, AMSU-A and ATMS orbital data files. However, several bias correction procedure requires solving multiple satellite regression equations. This requires a computer system to contain an internal library which has a software program to be called directly for solving multiple linear equations.

3.4.4 Calculations

Please refer to the flowcharts in section 3.2 for the detailed calculation steps to generate the MSU/AMSU/ATMS atmospheric layer temperature records.

3.4.5 Look-Up Table Description

Limb adjustment and frequency adjustment generated from the CRTM simulations are provided as look-up tables. At each grid point, there are frequency adjustment tables to adjust the MSU observations for channel 2, 3, and 4 from different satellites to their companion AMSU-A channels 5, 7, and 9, respectively. At each scan position, there are corresponding limb-adjustment terms to adjust the off-nadir radiances for AMSU-A channels 5, 7, and 9 and ATMS channels 6, 8, and 10 to near-nadir views.

3.4.6 Parameterization

N/A

3.4.7 Algorithm Output

Algorithm outputs are the products generated from the algorithm. Please refer to Section 2.1 and Table 2.1 for a detailed description on the algorithm outputs.

4. Test Datasets and Outputs

4.1 Test Input Datasets

Three research groups have developed the MLT CDR in previous investigations. These include SATR, University of Alabama at Huntsville (UAH), and Remote Sensing Systems (RSS). The test datasets here are the latest MLT versions from these groups, which include the UAH Version 6 CDR (Spencer et al. 2017), RSS Version 4.0 CDR (Mears et al. 2016), and the earlier STAR Version 4.1 CDR (Zou and Wang 2011). The Mean Layer Temperature - NOAA CDR v5.0 is compared to these test datasets for a discussion of reproducibility in the following subsections.

4.2 Test Output Analysis

4.2.1 Reproducibility

Figure 4-1 show ccomparisons of deseasonalized global mean anomaly time series for TMT, TUT, and TLS, respectively, between Mean Layer Temperature - NOAA CDR v5.0 and the test datasets during January 1979–June 2021. The Mean Layer Temperature - NOAA CDR v5.0 shows excellent agreement in varibility with the test datasets. This is because all of these datasets used microwave sounding channels with the same frequency for development of TMT, TUT, and TLS and these channels have the same sensitivity to the corresponding MLT changes. This result demonstrates the reproducibility of the MLT CDR for all TMT, TUT, and TLS. Note that agreement in variability among different datasets do not provide an accuracy estimate in trend detection for a specific dataset. Trend accuracies in a specific dataset shall be estimated by validations against absolute standards. When there are no standards such as in the case of MLT, accuracy shall be estimated based on the physical and mathematical validity of the merging algorithms and consistency of the recalibrated and bias corrected multiple satellites data records. This is discussed in the next subsection.

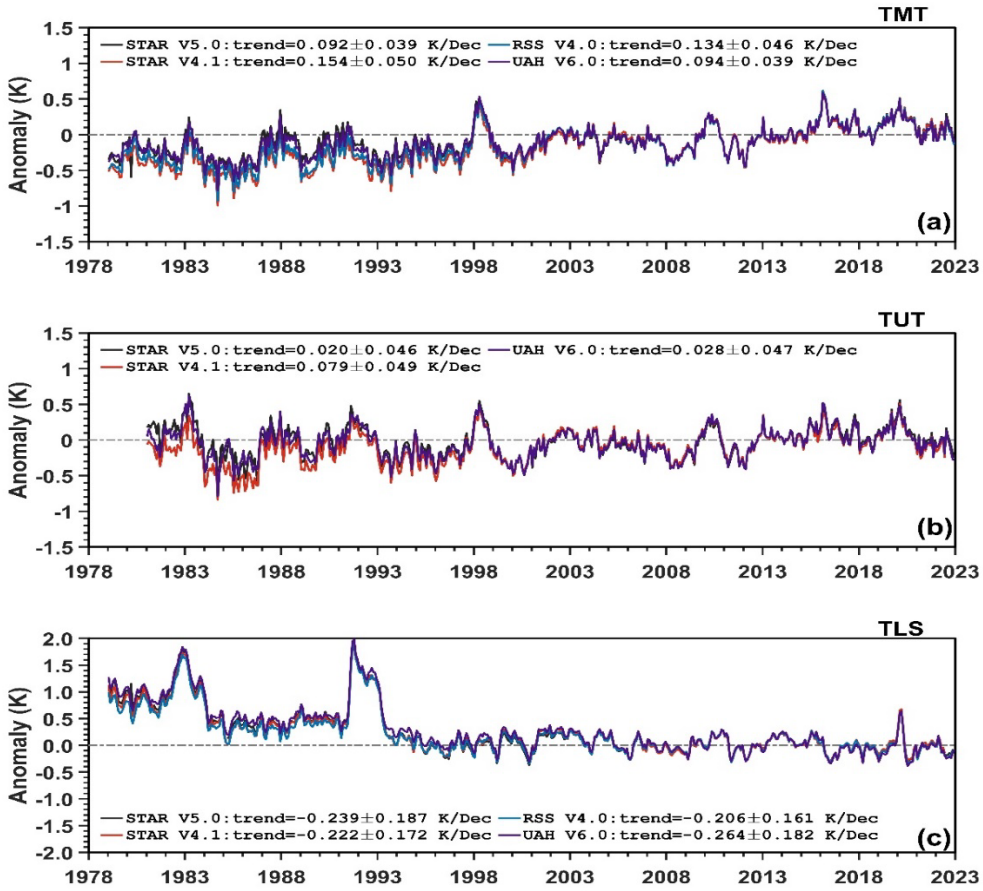

Figure 4-1. Deseasonalized global mean anomaly time series for Mean Layer Temperature - NOAA CDR v5.0, Mean Layer Temperature - NOAA CDR V4.1, UAH V6.0, and RSS V4.0 during January 1979–December 2022. a) TMT, b) TUT, and c) TLS.

4.2.2 Uncertainty and Accuracy

The MLT CDR has been mainly used for climate trend detection. Uncertainties in trend detection are divided into *structure uncertainty* and *internal uncertainty*. Structure uncertainty is caused by unknown calibration errors in instrument measurement. It could be estimated by comparing observations from different instrument types or the same data products but developed by different research groups. Internal uncertainties mainly come from errors in adjusting algorithms. A detailed analysis of internal uncertainties on various adjusting algorithms in Mean Layer Temperature - NOAA CDR v5.0 is given in Zou et al. (2023). Below only gives a summary of the internal uncertainty estimates for Mean Layer Temperature - NOAA CDR v5.0.

Uncertainty (accuracy) estimates in trend detection in Mean Layer Temperature - NOAA CDR v5.0 are separated into two periods: period of the reference time series from 2002 to present and the entire CDR period from late 1978 to present. For the reference time series, Zou et al. (2021) has discussed its accuracy in trend detection in detail. There are three foundations for this accuracy estimate: i) all satellites used in the reference time series are in sun-synchronous stable orbits so that no diurnal and other adjustments are needed; ii) all satellites in the reference time series have achieved high radiometric stability performance so that their inter-satellite difference trends are small; iii) all satellites used in the reference time series are calibrated independently so that their averages are statistically meaningful. With these characteristics, this trend accuracy can be estimated in Figure 3-8 for the merged (averaged) time series from independently-calibrated multiple satellite observations. Based on the measurement error analysis with small sampling size, accuracy of the averaged trends after satellite merging is expressed as $\pm\frac{\Delta}{2\sqrt{N}}$, where Δ (=0.048 K/decade) denotes the maximum relative drifting error, or spread of trends, and N (=2) the number of overlapping satellites. This results in a trend uncertainty (accuracy), or stability, of only 0.017 K/decade for the merged time series over periods with satellite overlaps. By assuming that a satellite without overlaps has a drifting error of 0.048 K/Decade while each of the two overlapping satellites has one-half of this drifting error, a trend uncertainty of 0.017K/Decade is also obtained for the entire reference period of the merged time series based on statistical simulations.

Zou et al. (2023) estimated the internal trend uncertainty for the entire CDR period from late 1978 to present. This internal uncertainty included those from recalibration, diurnal drift adjustment, error propagation from the reference time series to the earlier satellites, and an internal uncertainty of 0.012 K/decade from all other adjustments. Using statistical simulations, the uncertainty for the global mean TMT time series from late 1978 to present is obtained as 0.019 K/decade (Zou et al. 2023).

5. Practical Considerations

5.1 Numerical Computation Considerations

1. To speed up the generation of level-3 data (from swath scene brightness temperature to gridded temperature), multithread technique is employed in CDR development software code. This technique allows the CDR software to run faster on a computer system that has multiple CPUs or CPU with multiple cores. Multiple MSU/AMSU-A/ATMS level-1c files can be processed simultaneously to produce level-3 files with this approach.

2. Unqualified level-3 data: The monthly level-3 data of individual satellites may incur relatively larger errors in certain months. This may be caused by insufficient swath scene temperatures and invalid level-1c scan lines, etc, for the month. It may lead to outliers in the merged time series. To ensure high quality of dataset, all monthly level-3 files generated from the level-1c were sifted manually month by month before applying bias correction and merging algorithms.

5.2 Programming and Procedural Considerations

MSU/AMSU-A/ATMS MLT CDR software package does not implement any numerical model.

5.3 Quality Assessment and Diagnostics

The quality of the final products was evaluated in the following ways:

1. Inter-satellite biases for each satellite pair during their overlapping period are evaluated as an indicator of the product quality and accuracy of merging algorithms. Mean inter-satellite differences after bias correction were shown to be zero and standard deviations were minimized compared to those without bias corrections. These indicated high quality and accuracy of the merged products.

2. Monthly images of the layer temperatures for the entire observational period from 1978-present were put on the project website for a frequent check of possible data quality issues (see https://www.star.nesdis.noaa.gov/smcd/emb/mscat/imageBrowser.php). If outliers were found for a particular month, input data will be reexamined to find the root causes and then more rigorous quality controls on the input data will be implemented until the problem is resolved. Animation of monthly images show continuous changes of the climate event both locally and globally, indicting high quality of products.

5.4 Exception Handling

Exceptions considered in the MLT processing codes include:

1. ClassNotFound Exception will be reported and the system stops running when the code tries to load in a class but no definition for the class could be located due to misplacement of external libraries

2. OutOfMemory Exception will be identified when the system cannot allocate a block a memory. If this exception occurs, the system will report the exception and exit running

3. FileNotFound Exception will be reported and the system exits running when an ancillary file does not exist or inaccessible

4. EOF Exception will be reported when an end of file has been reached unexpectedly during file reading operations

5. IOException will be reported and the system stops running when a failed I/O operation, other than exceptions 3 and 4, occurs.

5.5 Algorithm Validation

As described in sections 4.1, 4.2 and 5.3.

5.6 Processing Environment and Resources

Table 5-1 lists the environment and resource requirements for the MSU/AMSU-A/ATMS MLT CDR processing codes.

Table 5-1. Processing environment and resource requirements.

Computer Hardware	Minimum Configuration: Processor: 2.0GHz Memory: 8G Disk Space 10 TB A system with multiple CPUs is preferred
Operating System	Linux or Windows
Programming Languages	JAVA Bash script
Compilers	Oracle JAVA Compiler
External Library	NetCDF-JAVA 4.6 Jscience 4.3
Storage Requirement	10 TB
Execution Time Requirement	Single CPU ~72 hours for 15 satellites Varied when using parallel computing

6. Assumptions and Limitations

6.1 Algorithm Performance

Algorithm performance for satellite merging was discussed in detail in Zou et al. (2023). Figures 3-5 to 3-17 and relevant discussions in this document also provided a summary on the algorithm performance. Key assumptions in the algorithm development were the use of the reference time series as an anchor in inter-satellite bias corrections. Algorithm performance was quite well and stable before 2018. Future dataset performance in trend detection relies on the sensor performance of the JPSS satellites after 2023.

6.2 Sensor Performance

After 2018, only ATMS instruments onboard JPSS satellites (SNPP and NOAA-20) are included in the reference time series in Mean Layer Temperature - NOAA CDR v5.0. As such, calibration drift in the ATMS sensor performance is critical in determining the total trends in the Mean Layer Temperature - NOAA CDR v5.0. Frequent monitoring, assessment and recalibration of the ATMS calibration drifts are required. This could be done by comparing the long-term time series between the JPSS satellites such as the SNPP and NOAA-20.

7. Future Enhancements

The merging algorithms for Mean Layer Temperature - NOAA CDR v5.0 were well described and justified with effective removal of inter-satellite biases before 2018. Future enhancements are to include more JPSS ATMS observations (such as NOAA-21) in the reference time series in the MLT CDR

8. References

Christy, J. R., R.W. Spencer, W.D. Braswell (2000). MSU tropospheric temperatures: Dataset construction and radiosonde comparisons. *J. Atmos. Oceanic. Technol.* 17:1153–1170

Goldberg, M.D., D.S. Crosby, L. Zhou (2001). The limb adjustment of AMSU-A observations: methodology and validation. *J. App. Meteor.* 40:70–83.

Goldberg, M. D., Kilcoyne, H., Cikanek, H., & Mehta, A. (2013). Joint Polar Satellite System: The United States next generation civilian polar-orbiting environmental satellite system. Journal of Geophysical Research: Atmospheres, 118(24), 13463– 13475. https://doi.org/10.1002/2013jd020389

Kidwell, K. B. (1998). NOAA polar orbiter data users guide. NOAA. Retrieved from http://webapp1.dlib.indiana.edu/virtual_disk_library/index.cgi/4284724/FID2496/podug/index.htm

Han, Y., van Delst P., Liu Q. , Weng F. , Yan B. , Treadon R. , and Derber J. (2006). JCSDA Community Radiative Transfer Model (CRTM)—version 1. NOAA Tech. Rep., NESDIS 122, 40 pp.

Lu, Q., and W. Bell (2014). Characterizing channel center frequencies in AMSU-A and MSU microwave sounding instruments. *J. Atmos. Oceanic Technol*. **31**, 1713–1732.

Mears, C. A., and F. J. Wentz, 2016: Sensitivity of satellite-derived tropospheric temperature trends to the diurnal cycle adjustment. *J. Clim*. **29**, 3629–3646.

Mo, T., 1995: Calibration of the advanced microwave sounding unit-A for NOAA-K, NOAA Tech. Rep. NESDIS 85, Natl. Oceanic and Atmos. Admin., Washington, DC.

Mo, T., 1996: Prelaunch calibration of the Advanced Microwave Sounding Unit-A for NOAA-K, IEEE Trans. On Microwave Theory and Techniques, 44(8), 1460-1469.

Robel, J., & Graumann, A. (2014). NOAA KLM user's guide. Retrieved from https://webapp1.dlib.indiana.edu/virtual_disk_library/index.cgi/2790181/FID1497/Klm

Spencer, R.W., J. R. Christy, W. D. Braswell, 2017: UAH version 6 global satellite temperature products: Methodology and results, Asia-Pac. J. Atmos. Sci. 53, 121-130.

Wang, Wenhui, Cheng-Zhi Zou, 2014: AMSU-A-Only Atmospheric Temperature Data Records from the Lower Troposphere to the Top of the Stratosphere. *J. Atmos. Oceanic Technol.*, 31,

Weng, F., Zou, X., Wang, X., Yang, S., & Goldberg, M. D. (2012). Introduction to Suomi national polar-orbiting partnership advanced technology microwave sounder for numerical weather prediction and tropical cyclone applications. Journal of Geophysical Research, 117(D19), D19112. https://doi.org/10.1029/2012JD018144808-825, DOI: 10.1175/JTECH-D-13-00134.1

Zhang, K., Zhou, L., Goldberg, M., Liu, X., Wolf, W., Tan, C., & Liu, Q. (2017). A methodology to adjust ATMS observations for limb effectand its applications. J. Geophys. Res.: Atmosphere, **122**, 11347–11356. https://doi.org/10.1002/2017JD026820

Zou, C.-Z., *et al.* (2006). Recalibration of microwave sounding unit for climate studies using simultaneous nadir overpasses. *J. Geophys. Res.*, 111(D19), D19114

Zou, C.-Z., *et al.* (2009). Error structure and atmospheric temperature trends in observations from the Microwave Sounding Unit. *Journal of Climate*, 22(7), 1661-1681

Zou, C.-Z., and W. Wang (2010). Stability of the MSU-derived atmospheric temperature trend. *Journal of Atmospheric and Oceanic Technology*, 27(11), 1960-1971

Zou, C.-Z., and W. Wang (2011). Intersatellite calibration of AMSU-A observations for weather and climate applications. *J. Geophys. Res.,* 116(D23), D23113

Zou, C.-Z. and W. Wang (2013). MSU/AMSU Radiance Fundamental Climate Data Record Calibrated Using Simultaneous Nadir Overpasses Climate Algorithm Theoretical Basis Document (C-ATBD), NOAA/NESDIS

Zou, C.-Z., M. Goldberg, and X. Hao (2018), New generation of U.S. satellite microwave sounder achieves high radiometric stability performance for reliable climate change detection, Science Advances, 4(10), eaau0049, doi: 10.1126/sciadv.aau0049.

Zou, C.-Z. et al. (2020), The Reprocessed Suomi NPP Satellite Observations, Remote Sens. (12)18, 2891, doi:10.3390/rs12182891.

Zou, C.-Z. et al. (2021), Post-millennium atmospheric temperature trends observed from satellites in stable orbits, Geophysical Research Letters, (48)13, e2021GL093291. https://doi.org/10.1029/2021GL093291

Zou, C.-Z., Xu, H., Hao, X., and Liu, Q. (2023). Mid-tropospheric layer temperature record derived from satellite microwave sounder observations with backward merging approach. Journal of Geophysical Research: Atmospheres, 128, e2022JD037472. https://doi.org/10.1029/2022JD037472.

Appendix A. Acronyms and Abbreviations

Acronym or Abbreviation	Meaning
AMSU	Advanced Microwave Sounding Unit
ATMS	Advanced Technology Microwave Sounder
CATBD	Climate Algorithm Theoretical Basis Document
CDR	Climate Data Record
CDRP	Climate Date Record Program
CRTM	Community Radiative Transfer Model
EUMETSAT	European Organisation for the Exploitation of Meteorological Satellites
FCDR	Fundamental Climate Data Record
FOV	Field of View
GPSRO	Global Positioning System Radio Occultation
IFOV	Instantaneous Field of View
IMICA	Integrated Microwave Inter-Calibration Approach
MERRA	NASA's Modern-Era Retrospective Analysis for Research and Applications
MetOp-A	The European Meteorological Operational satellite program-A
MSU	Microwave Sounding Unit
NCEI	National Centers for Environmental Information
NESDIS	National Environmental Satellite, Data, and Information Services
NetCDF	Network Common Data Form
NASA	National Aeronautics and Space Administration
NOAA	National Oceanic and Atmospheric Administration
PRT	Platinum Resistance Thermometer
RSS	Remote Sensing Systems
SNO	Simultaneous Nadir Overpass
STAR	Center for Satellite Applications and Research
TCDR	Thematic Climate Data Record
TLT	Temperature of lower-troposphere
TLS	Temperature of lower-stratosphere
TMT	Temperature of mid-troposphere
TUT	Temperature of upper-troposphere
UAH	University of Alabama at Huntsville

Disclaimer: The views, opinions, and findings contained in this report are those of the authors and should not be construed as an official NOAA or U.S. Government position, policy, or decision.